**České vysoké učení technické v Praze, Fakulta strojní**
**Ústav technické matematiky**

**Czech Technical University in Prague, Faculty of Mechanical Engineering**
**Department of Technical Mathematics**

Doc. RNDr. Pavel Burda, CSc.

# Apriorní a aposteriorní odhady chyby v metodě konečných prvků pro Navierovy-Stokesovy rovnice a aplikace v úlohách se singularitami

# A Priori and A Posteriori Error Estimates in the Finite Element Method for Navier-Stokes Equations and Applications in Problems with Singularities

Praha, 2005

## Summary

At present finite element method is very well established technique to solve various practical problems. Application of the finite element method (FEM) in engeneering has made a rapid progress, and it is widely used in industry as well as in research centers today.

Whereas the application of the FEM in the structural mechanics seems to be now clear enough for solving common tasks, and only special problems remain to be resolved, in fluid dynamics there are still many open and not well handled problems. One of them is reliable modelling of flows in channels or tubes with abrupt changes of the diameter, which appear often in engineering practice. The goal of this work is to construct the FEM solution in the vicinity of these corners as precise as desired.

We present two ways for getting desired precision of the FEM solution in the vicinity of corners. Both make use of qualitative properties of the mathematical model of flow. As a mathematical model we accept the Navier-Stokes equations for incompressible fluids.

The first approach makes use of a posteriori error estimates of the FEM solution which are carefully derived to trace the quality of the solution. Especially the constant in the a posteriori estimate is investigated with care. Then we use the adaptive strategy to improve the mesh and thus to improve the FEM solution. We present some numerical results.

The second approach stands on two legs. One is the asymptotic behaviour of the exact solution of the NSE in the vicinity of the corner. This is obtained using some symmetry of the principal part of the Stokes equation, and application of the Fourier transform. Second leg is the a priori error estimate of the FEM solution where we estimate the seminorm of the exact solution by means of the above obtained asymptotics. These ideas allow to derive an algorithm for designing the FEM mesh in advance (a priori). On the mesh we then obtain the solution with desired precision also in the vicinity of the corner though there is a singularity here. This approach offers quite cheap and precise computing of selected problems. Numerical results are demonstrated on two examples.

Finally we discuss main achievements and topics for further research.

# Souhrn

V současné době metoda konečných prvků představuje velmi dobře propracovanou metodiku pro řešení nejrůznějších praktických úloh. Užití metody konečných prvků (MKP) v inženýrské praxi prodělalo v posledních 35 letech významný pokrok, a v současné době je metoda široce využívána v průmyslu i v řadě netechnických oborů.

Zatímco v úlohách pevné fáze se aplikace MKP zdá být dostatečně propracována, a zbývá dořešit jen některé speciální problémy, v dynamice tekutin je stále řada otevřených problémů jak v numerické teorii tak v aplikacích. Jedním z nich je spolehlivé modelování proudění tekutin v kanálech a trubicích s náhlou změnou průměru, což je časté jak v technických aplikacích tak např v modelování proudění krve v cévních náhradách. Cílem této práce je konstruovat konečněprvkové řešení v blízkosti takových rohů tak přesně jak je vyžadováno.

Uvádíme dva způsoby pro získání požadované přesnosti řešení MKP v blízkosti rohů. Oba využívají kvalitativní vlastnosti matematického modelu proudění. Jako matematický model přijímáme Navierovy-Stokesovy rovnice pro nestlačitelnou tekutinu.

První způsob využívá aposteriorní odhady MKP řešení. Ty jsou pečlivě odvozeny za účelem vystopovat kvalitu řešení. Specielně konstanta v aposteriorním odhadu je pečlivě zkoumána. Je pak použita adaptivní strategie ke zlepšení sítě a tím ke zlepšení přesnosti FEM řešení. Uvádíme některé numerické výsledky.

Druhý přístup stojí na dvou sloupech. Jedním je asymptotické chování exaktního řešení Navierových-Stokesových rovnic v blízkosti rohu. To se získá užitím jisté symetrie vůdčí části Stokesových rovnic, a aplikací Fourierovy transformace k převedení na jednodimensionální problém. Druhým sloupem je apriorní odhad MKP řešení, kde odhadujeme seminormu exaktního řešení pomocí zmíněného asymptotického odhadu. Tento přístup umožňuje odvodit algoritmus pro navržení MKP sítě před vlastním výpočtem. Na takové síti pak obdržíme řešení s předepsanou přesností v okolí rohu, kde exaktní řešení má singularitu. Tento přístup umožňuje velice levně získat dostatečně precisní řešení. Na dvou aplikacích ukazujeme numerické výsledky.

V závěru jsou diskutovány hlavní dosažené výsledky a náměty pro další výzkum.

## Klíčová slova:

Metoda konečných prvků, Navierovy-Stokesovy rovnice, nestlačitelná tekutina, apriorní odhad, aposteriorní odhad, singularita.

## Key Words:

Finite element method, Navier-Stokes equations, inconpressible flow, a priori estimate, a posteriori estimate, singularity.

# Contents


**1 Introduction** **6**

**2 Navier-Stokes equations for incompressible viscous fluids** **7**
2.1 Unsteady two-dimensional flow . . . . . . . . . . . . . . . . . . . . . . . . . . . 7
2.2 Steady 2D Navier-Stokes problem . . . . . . . . . . . . . . . . . . . . . . . . . 7
2.3 Steady 2D Stokes problem . . . . . . . . . . . . . . . . . . . . . . . . . . . . 8
2.4 Unsteady axisymmetric flow . . . . . . . . . . . . . . . . . . . . . . . . . . . 8
2.5 Variational formulation of Navier-Stokes equations . . . . . . . . . . . . . . . . . 8

**3 Finite element method for Navier-Stokes equations** **10**
3.1 Function spaces for velocity and pressure approximation . . . . . . . . . . . . . 10
3.2 Hood-Taylor finite elements . . . . . . . . . . . . . . . . . . . . . . . . . . . 10

**4 Asymptotic behaviour of the solution near corners** **12**
4.1 Solution of Navier-Stokes equations in the axisymmetric case . . . . . . . . . . . 12
4.2 Asymptotics of steady Navier-Stokes flow near the corner . . . . . . . . . . . . . 13

**5 A posteriori error estimates for the Stokes equation** **16**
5.1 The Stokes problem and finite element solution . . . . . . . . . . . . . . . . . . 16
5.2 A posteriori error estimate for the Stokes problem . . . . . . . . . . . . . . . . . 16
5.3 A posteriori estimates for 2D steady Navier-Stokes equations . . . . . . . . . . . 17
5.4 Determination of the constant C . . . . . . . . . . . . . . . . . . . . . . . . . 18
5.5 Numerical results and application of estimates to the construction of adaptive meshes . . . . . . . . . . . . . . . . . . . . . . . . . . . . . . . . . . . . . 18
5.6 Conclusions . . . . . . . . . . . . . . . . . . . . . . . . . . . . . . . . . . . 20

**6 Application of a priori error estimates for Navier-Stokes equations** **21**
6.1 Algorithm for generation of computational mesh . . . . . . . . . . . . . . . . . . 21
6.2 Geometry and design of the mesh . . . . . . . . . . . . . . . . . . . . . . . . . 22
6.3 Measuring of error . . . . . . . . . . . . . . . . . . . . . . . . . . . . . . . . 23
6.4 Numerical results . . . . . . . . . . . . . . . . . . . . . . . . . . . . . . . . 24

**7 Conclusion** **27**

**8 References** **28**

**9 Curriculum Vitae** **30**

# 1 Introduction

At present finite element method is very well established technique to solve various practical problems. Application of the finite element method (FEM) in engeneering has made a rapid progress, and it is widely used in industry as well as in research centers today.

Whereas the application of the FEM in the structural mechanics seems to be now clear enough for solving common tasks, and only special problems remain to be resolved, in fluid dynamics there are still many open and not well handled problems. One of them is reliable modelling of flows in channels or tubes with abrupt changes of the diameter, which appear often in engineering practice. The goal of this work is to construct the FEM solution in the vicinity of these corners as precise as desired.

We present two ways for getting desired precision of the FEM solution in the vicinity of corners. Both make use of qualitative properties of the mathematical model of flow. As a mathematical model we accept the Navier-Stokes equations (NSE) for incompressible fluids.

The first approach makes use of a posteriori error estimates of the FEM solution which is carefully derived to trace the quality of the solution. Especially the constant in the a posteriori estimate is investigated with care. Then we use the adaptive strategy to improve the mesh and thus to improve the FEM solution.

The second approach stands on two legs. One is the asymptotic behaviour of the exact solution of the NSE in the vicinity of the corner. This is obtained using some symmetry of the principal part of the Stokes equation, and application of the Fourier transform. Second leg is the a priori error estimate of the FEM solution where we estimate the seminorm of the exact solution by means of the above obtained asymptotics. These ideas allow to derive an algorithm for designing the FEM mesh in advance (a priori). On the mesh we then obtain the solution with desired precision also in the vicinity of the corner though there is a singularity here.

The structure of the work is as follows. Navier-Stokes equations as a model of flow of an incompressible viscous fluid are introduced in Chapter 2. In Chapter 3, FEM formulation of the Navier-Stokes problem is described. Capter 4 is devoted to the asymptotic behaviour of the exact solution of the Stokes and Navier-Stokes equations in the neighborhood of corners.

Chapter 5 deals with the a posteriori error estimates, with the determination of the constant $C$ in it, and we present some numerical results. Chapter 6 is devoted more to the aspect of accuracy of the FEM applied to flow in channels with sharp nonconvex inner corners. It deals with the application of a priori error estimates of the FEM to mesh generation. This approach offers quite cheap and precise computing of selected problems. Numerical results are demonstrated on two examples. In Chapter 7 we discuss main achievements and topics for further research.

# 2 Navier-Stokes equations for incompressible viscous fluids

Let $\Omega$ be an open bounded domain in $\mathbb{R}^2$ filled with a fluid, and let $\Gamma$ be its Lipschitz continuous boundary. The generic point of $\mathbb{R}^2$ is denoted by $\mathbf{x} = (x_1, x_2)^T$ considered in meters, and $t$ denotes time variable considered in seconds.

## 2.1 Unsteady two-dimensional flow

We deal with isothermal flow of Newtonian viscous fluids with constant density. Such flow is modelled by the Navier-Stokes system of partial differential equations (nonconservative form):

$$\rho\left(\frac{\partial \mathbf{u}}{\partial t} + (\mathbf{u}\cdot\nabla)\mathbf{u}\right) - \mu\Delta\mathbf{u} + \nabla p_r = \rho\,\mathbf{f} \quad \text{in } \Omega\times[0,T] \tag{2.1}$$

$$\nabla\cdot\mathbf{u} = 0 \quad \text{in } \Omega\times[0,T] \tag{2.2}$$

where

- $\mathbf{u} = (u_1, u_2)^T$ denotes the vector of flow velocity, in $m/s$, being a function of $\mathbf{x}$ and $t$
- $p_r$ denotes the pressure considered in $Pa$, which is a function of $\mathbf{x}$ and $t$
- $\rho$ denotes the density of the fluid considered in $kg/m^3$
- $\mu$ denotes the dynamic viscosity of the fluid, in $Pa\cdot s$, supposed to be constant
- $\mathbf{f} = \mathbf{f}(\mathbf{x}, t)$ is the density of volume forces per mass unit considered in $N/m^3$

Dividing both sides of the momentum equation (2.1) by $\rho$ and leaving the continuity equation (2.2) unchanged we obtain

$$\frac{\partial \mathbf{u}}{\partial t} + (\mathbf{u}\cdot\nabla)\mathbf{u} - \nu\Delta\mathbf{u} + \nabla p = \mathbf{f} \quad \text{in } \Omega\times[0,T] \tag{2.3}$$

$$\nabla\cdot\mathbf{u} = 0 \quad \text{in } \Omega\times[0,T] \tag{2.4}$$

where

- $p = \frac{p_r}{\rho}$ denotes the pressure divided by the density considered in $Pa\cdot m^3/kg$
- $\nu = \frac{\mu}{\rho}$ denotes the kinematic viscosity of the fluid considered in $m^2/s$

The system is supplied with the initial condition

$$\mathbf{u} = \mathbf{u}_0 \ \text{ in } \Omega,\ t = 0 \tag{2.5}$$

where $\nabla\cdot\mathbf{u}_0 = 0$, and with the boundary conditions

$$\mathbf{u} = \mathbf{g} \ \text{ on } \Gamma_g\times[0,T] \tag{2.6}$$

$$-\nu(\nabla\mathbf{u})\mathbf{n} + p\mathbf{n} = \mathbf{0} \ \text{ on } \Gamma_h\times[0,T] \tag{2.7}$$

where

- $\Gamma_g$ and $\Gamma_h$ are two subsets of $\Gamma$ satisfying $\overline{\Gamma} = \overline{\Gamma}_g \cup \overline{\Gamma}_h,\ \mu_{\mathbb{R}^1}(\Gamma_g\cap\Gamma_h) = 0$
- $\mathbf{n}$ denotes the unit outer normal vector to the boundary $\Gamma$.

Introduced $\mathbf{g}$ is a given function of $\mathbf{x}$ and $t$ satisfying in the case of $\Gamma = \Gamma_g$ for all $t \in [0,T]$

$$\int_\Gamma \mathbf{g}\cdot\mathbf{n}\,\mathrm{d}\Gamma = 0$$

## 2.2 Steady 2D Navier-Stokes problem

For the case of steady two-dimensional flow, the Navier-Stokes equations are reduced to

$$(\mathbf{u}\cdot\nabla)\mathbf{u} - \nu\Delta\mathbf{u} + \nabla p = \mathbf{f} \quad \text{in } \Omega \tag{2.8}$$

$$\nabla\cdot\mathbf{u} = 0 \quad \text{in } \Omega \tag{2.9}$$

and boundary conditions to

$$\mathbf{u} = \mathbf{g} \ \text{ on } \Gamma_g \tag{2.10}$$

$$-\nu(\nabla\mathbf{u})\mathbf{n} + p\mathbf{n} = \mathbf{0} \ \text{ on } \Gamma_h \tag{2.11}$$

## 2.3 Steady 2D Stokes problem

In case of the Stokes flow the first (nonlinear) term in (4.6) is omitted:

$$\begin{aligned} -\nu\Delta\mathbf{u} + \nabla p &= \mathbf{f} \quad \text{in } \Omega && (2.12)\\ \nabla\cdot\mathbf{u} &= 0 \quad \text{in } \Omega && (2.13) \end{aligned}$$

and boundary conditions are the same as in (2.10), (2.11).

## 2.4 Unsteady axisymmetric flow

Let us now consider the system of Navier-Stokes equations for incompressible viscous fluid in three dimensions, cf. [20]. Performing transformation of the cartesian system of coordinates $\{x_1, x_2, x_3\}$ into the cylindrical system of coordinates $\{r, \varphi, z\}$ where

$$x_1 = r\cos\varphi;\;\; x_2 = r\sin\varphi;\;\; x_3 = z,$$

and considering axialy symmetric flow, i.e. variables are independent of $\varphi$, we obtain Navier-Stokes equations in the form (cf. e.g. [8])

$$\begin{aligned} \frac{\partial u}{\partial t} + v\frac{\partial u}{\partial r} + u\frac{\partial u}{\partial z} - \nu\left(\frac{\partial^2 u}{\partial r^2} + \frac{1}{r}\frac{\partial u}{\partial r} + \frac{\partial^2 u}{\partial z^2}\right) + \frac{\partial p}{\partial z} &= f_z \quad \text{in } \Omega\times[0,T] && (2.14)\\ \frac{\partial v}{\partial t} + v\frac{\partial v}{\partial r} + u\frac{\partial v}{\partial z} - \nu\left(\frac{\partial^2 v}{\partial r^2} + \frac{1}{r}\frac{\partial v}{\partial r} - \frac{v}{r^2} + \frac{\partial^2 v}{\partial z^2}\right) + \frac{\partial p}{\partial r} &= f_r \quad \text{in } \Omega\times[0,T] && (2.15)\\ \frac{\partial v}{\partial r} + \frac{v}{r} + \frac{\partial u}{\partial z} &= 0 \quad \text{in } \Omega\times[0,T] && (2.16) \end{aligned}$$

where

- $u = u(\mathbf{x}, t)$ is the axial component of velocity (direction of $z$-coordinate), in $m/s$
- $v = v(\mathbf{x}, t)$ is the radial component of velocity (direction of $r$-coordinate), in $m/s$
- $\mathbf{f} = \mathbf{f}(\mathbf{x}, t) = (f_z, f_r)^T$ is the density of volume forces per mass unit, in $N/m^3$

Equations (2.14)-(2.16) govern the axisymmetric flow in a domain $\Omega \subset \mathbb{R}^2$, where the generic point of $\mathbb{R}^2$ is now denoted by $\mathbf{x} = (z, r)^T$ for arbitrary $\varphi$.

## 2.5 Variational formulation of Navier-Stokes equations

Let $L_2(\Omega)$ be the space of square integrable functions on $\Omega$, and let $L_2(\Omega)/\mathbb{R}$ be the space of functions in $L_2(\Omega)$ ignoring an additive constant. Let $H^1(\Omega)$ and $H^1_0(\Omega)$ be the Sobolev spaces defined as

$$\begin{aligned} H^1(\Omega) &\equiv \left\{v \mid v \in L^2(\Omega), \frac{\partial v}{\partial x_i} \in L^2(\Omega), i = 1, 2\right\}\\ H^1_0(\Omega) &\equiv \left\{v \mid v \in H^1(\Omega), \mathbf{Tr}\ v = 0\right\} \end{aligned}$$

where $\mathbf{Tr}$ is the trace operator $\mathbf{Tr}:\ H^1(\Omega) \longrightarrow L_2(\Gamma)$, and derivatives are considered in the weak sense.

The inner product and norm in the space $L_2(\Omega)$ are defined as

$$(u, v)_{L_2(\Omega)} \equiv \int_\Omega uv \,\mathrm{d}\Omega \qquad \|v\|^2_{L_2(\Omega)} \equiv \int_\Omega v^2 \mathrm{d}\Omega$$

and the norm of function $v$ in the Sobolev space $H^1(\Omega)$ is considered as

$$\|v\|^2_{H^1(\Omega)} \equiv \int_\Omega \left( v^2 + \sum_{k=1}^{2} \left( \frac{\partial v}{\partial x_k} \right)^2 \right) \mathrm{d}\Omega$$

Sometimes, the notation $\|\cdot\|_{L_2(\Omega)}$ is shortened to $\|\cdot\|_0$ and $\|\cdot\|_{H^1(\Omega)}$ to $\|\cdot\|_1$. Similarly, the notation $(u,v)_{L_2(\Omega)}$ is shortened to $(u,v)_0$.

Let us define vector function spaces $V_g$ and $V$ by

$$\begin{aligned} V_g &\equiv \left\{ \mathbf{v} = (v_1, v_2)^T \mid \mathbf{v} \in [H^1(\Omega)]^2; \mathbf{Tr}\ v_i = g_i, i = 1,2 \right\} \\ V &\equiv \left\{ \mathbf{v} = (v_1, v_2)^T \mid \mathbf{v} \in [H^1_0(\Omega)]^2 \right\} \end{aligned}$$

Let us note, that the norm of vector function $\mathbf{v}$ in the spaces $V_g$ and $V$ is then

$$\|\mathbf{v}\|^2_{[H^1(\Omega)]^2} \equiv \sum_{i=1}^{2} \int_\Omega \left( v_i^2 + \sum_{k=1}^{2} \left( \frac{\partial v_i}{\partial x_k} \right)^2 \right) \mathrm{d}\Omega$$

and the norm of vector function $\mathbf{v}$ in the space $[L_2(\Omega)]^2$ is

$$\|\mathbf{v}\|^2_{[L_2(\Omega)]^2} \equiv \sum_{i=1}^{2} \int_\Omega v_i^2 \mathrm{d}\Omega$$

The *weak unsteady Navier-Stokes problem* means seeking of $\mathbf{u}(t) = (u_1(t), u_2(t))^T \in V_g$ and $p(t) \in L_2(\Omega)/\mathbb{R}$ satisfying for any $t \in [0,T]$, and $\forall\ \mathbf{v} \in V$ and $\forall\ \psi \in L^2(\Omega)$:

$$\int_\Omega \frac{\partial \mathbf{u}}{\partial t} \cdot \mathbf{v} \mathrm{d}\Omega + \int_\Omega (\mathbf{u} \cdot \nabla)\mathbf{u} \cdot \mathbf{v} \mathrm{d}\Omega + \nu \int_\Omega \nabla \mathbf{u} : \nabla \mathbf{v} \mathrm{d}\Omega - \int_\Omega p \nabla \cdot \mathbf{v} \mathrm{d}\Omega = \int_\Omega \mathbf{f} \cdot \mathbf{v} \mathrm{d}\Omega \tag{2.17}$$

$$\int_\Omega \psi \nabla \cdot \mathbf{u} \mathrm{d}\Omega = 0 \tag{2.18}$$

$$\mathbf{u} - \mathbf{u}_g \in V. \tag{2.19}$$

The operation $\nabla \mathbf{u} : \nabla \mathbf{v}$ is defined as

$$\nabla \mathbf{u} : \nabla \mathbf{v} \equiv \frac{\partial u_x}{\partial x}\frac{\partial v_x}{\partial x} + \frac{\partial u_x}{\partial y}\frac{\partial v_x}{\partial y} + \frac{\partial u_y}{\partial x}\frac{\partial v_y}{\partial x} + \frac{\partial u_y}{\partial y}\frac{\partial v_y}{\partial y}$$

Similarly, the *weak steady Navier-Stokes problem* reads:
Seek $\mathbf{u} = (u_1, u_2)^T \in V_g$ and $p \in L_2(\Omega)/\mathbb{R}$ satisfying $\forall\ \mathbf{v} \in V$ and $\forall\ \psi \in L^2(\Omega)$:

$$\int_\Omega (\mathbf{u} \cdot \nabla)\mathbf{u} \cdot \mathbf{v} \mathrm{d}\Omega + \nu \int_\Omega \nabla \mathbf{u} : \nabla \mathbf{v} \mathrm{d}\Omega - \int_\Omega p \nabla \cdot \mathbf{v} \mathrm{d}\Omega = \int_\Omega \mathbf{f} \cdot \mathbf{v} \mathrm{d}\Omega \tag{2.20}$$

$$\int_\Omega \psi \nabla \cdot \mathbf{u} \mathrm{d}\Omega = 0 \tag{2.21}$$

$$\mathbf{u} - \mathbf{u}_g \in V. \tag{2.22}$$

In case of the *weak steady Stokes problem* instead of (2.20) we require

$$\nu \int_\Omega \nabla \mathbf{u} : \nabla \mathbf{v} \mathrm{d}\Omega - \int_\Omega p \nabla \cdot \mathbf{v} \mathrm{d}\Omega = \int_\Omega \mathbf{f} \cdot \mathbf{v} \mathrm{d}\Omega \tag{2.23}$$

# 3 Finite element method for Navier-Stokes equations

Let us divide the domain $\Omega$ (supposed now polygonal) into $N$ elements $T_K$ of a triangulation $\mathcal{T}$ such that

$$\begin{aligned} \bigcup_{K=1}^{N} \overline{T}_K &= \overline{\Omega} \\ \mu_{\mathbb{R}^2}\left(T_K \cap T_L\right) &= 0, K \neq L \end{aligned}$$

Let $h_K$ mean the largest distance in element $T_K$.

## 3.1 Function spaces for velocity and pressure approximation

To solve the Navier-Stokes equations, different polynomial approximation for velocities and for pressure are usually chosen. Equal order approximation is easy to implement, but pressure exhibits instability. Approximation with different order is more suitable for practical computing, cf. [4].

I. Babuška and F. Brezzi introduced a condition (also called *inf-sup* condition) limitting the choice of combinations of approximation

$$\exists_{C_B>0,const.}\ \forall_{q_h\in Q_h}\ \exists_{\mathbf{v}_h\in V_{gh}}\ (q_h, \nabla\cdot\mathbf{v}_h)_0 \geq C_B\|q_h\|_0\|\mathbf{v}_h\|_1 \tag{3.1}$$

where $Q_h$ and $V_{gh}$ are the function spaces for approximation of pressure and velocity. Condition (3.1) is important for stability. It is satisfied e.g. for Taylor-Hood elements we use.

## 3.2 Hood-Taylor finite elements

In this paper we apply Hood-Taylor finite elements on triangles and quadrilaterals. Values of velocity are aproximated in corner nodes and in midsides, and values of pressure in corner nodes (Figure 3.1). It corresponds to the following function spaces on element $T_K$:

- *triangle*

$$\begin{aligned} v_i &\in P_2(T_K),\ i=1,2, \quad \text{i.e. polynomial of the second order} \\ p &\in P_1(T_K) \quad \text{i.e. linear polynomial} \end{aligned}$$

- *quadrilateral*

$$\begin{aligned} v_i &\in Q_2(T_K),\ i=1,2, \quad \text{i.e. polynomial of the second order for each coordinate} \\ p &\in Q_1(T_K) \quad \text{i.e. bilinear polynomial} \end{aligned}$$

Let us employ the notation

$$R_m(\overline{T_K}) = \begin{cases} P_m(\overline{T_K}), & \text{if } T_K \text{ is a triangle} \\ Q_m(\overline{T_K}), & \text{if } T_K \text{ is a quadrilateral} \end{cases} \tag{3.2}$$

and let $\mathcal{C}(\overline{\Omega})$ denote the space of continuous functions on $\overline{\Omega}$.

Application of Hood-Taylor finite elements leads to the final approximation on the domain $\Omega$ satisfying $\mathbf{u}_h \in V_{gh}$ and $p_h \in Q_h$ where

$$\begin{aligned} V_{gh} = \Big\{ &\mathbf{v}_h = (v_{h_1}, v_{h_2})^T \in [\mathcal{C}(\overline{\Omega})]^2;\ v_{h_i}\,|_{T_K} \in R_2(\overline{T_K}),\ K=1,\ldots,N,\ i=1,2, \\ &\mathbf{v}_h = \mathbf{g} \text{ in nodes on } \Gamma \Big\} \end{aligned} \tag{3.3}$$

$$Q_h = \Big\{ \psi_h \in \mathcal{C}(\overline{\Omega});\ \psi_h\,|_{T_K} \in R_1(\overline{T_K}),\ K=1,\ldots,N \Big\} \tag{3.4}$$

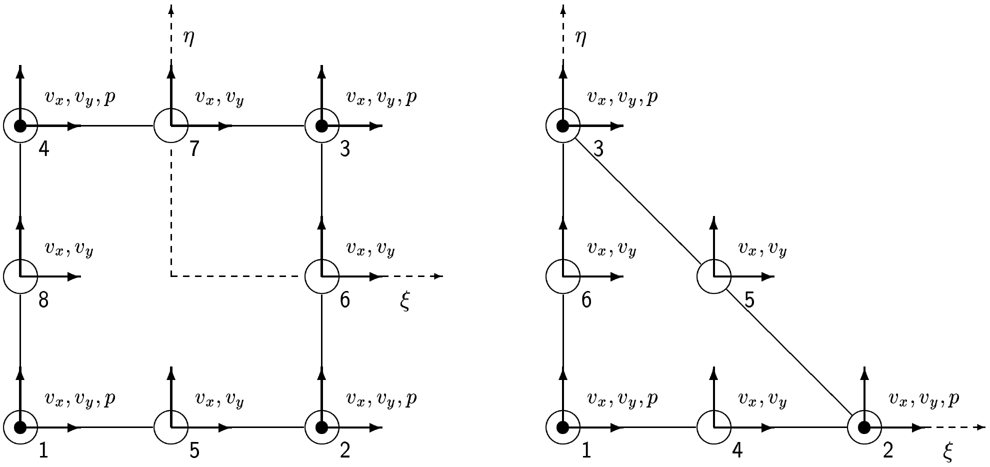


Fig. 3.1: Hood-Taylor reference elements

We also need the space

$$V_h = \Big\{ \mathbf{v}_h = (v_{h_1}, v_{h_2})^T \in [\mathcal{C}(\overline{\Omega})]^2;\ v_{h_i}\,|_{T_K} \in R_2(\overline{T_K}),\ K = 1, \ldots, N,\ i = 1, 2, \qquad \mathbf{v}_h = \mathbf{0} \text{ in nodes on } \Gamma \Big\} \tag{3.5}$$

Since these function spaces satisfy $V_{gh} \subset V_g$, $V_h \subset V$, and $Q_h \subset L_2(\Omega)/\mathbb{R}$ for prescribed arbitrary value of pressure (e.g. $p_h = 0$) in one node, we can introduce *approximate steady Navier-Stokes problem*:

Seek $\mathbf{u}_h \in V_{gh}$ and $p_h \in Q_h$ satisfying

$$\int_\Omega (\mathbf{u}_h \cdot \nabla)\mathbf{u}_h \cdot \mathbf{v}_h \mathrm{d}\Omega + \nu \int_\Omega \nabla \mathbf{u}_h : \nabla \mathbf{v}_h \mathrm{d}\Omega - \int_\Omega p_h \nabla \cdot \mathbf{v}_h \mathrm{d}\Omega = \int_\Omega \mathbf{f} \cdot \mathbf{v}_h \mathrm{d}\Omega,\ \forall \mathbf{v}_h \in V_h \tag{3.6}$$

$$\int_\Omega \psi_h \nabla \cdot \mathbf{u}_h \mathrm{d}\Omega = 0,\ \forall \psi_h \in Q_h \tag{3.7}$$

$$\mathbf{u}_h - \mathbf{u}_{gh} \in V_h \tag{3.8}$$

where $\mathbf{u}_{gh} \in V_{gh}$ is the projection of $\mathbf{u}_g$ onto the space $V_{gh}$.

Similarly we define *approximate steady Stokes problem*, just omitting the first term in (3.6).

Using the shape regular triangulation and refining the mesh such that $h_{max} \to 0$ where

$$h_{max} = \max_K h_K,$$

the solution of the approximated problem converges to the solution of the continuous problem (for more see e.g. [4]).

# 4 Asymptotic behaviour of the solution near corners

We are concerned with numerical solution of flow of incompressible fluid in tubes with abrupt changes of diameter. We study the axisymmetric flow governed by the Navier-Stokes equations. First concern is the asymptotic behaviour of the solution near the corners. Fundamental part of this chapter is based on the paper [5].

In next chapters we deal with the numerical solution of the flow in a tube with sharp changes of diameter. In plane flow, the finite element method has been succesfully used e.g. in [27]. The singularity at the corner needs appropriate local refinement of the mesh.

To solve axisymmetric flow we used also the MAC method for space discretization. Numerical results for pulsatile axisymmetric flow were published in [8], [9], [10].

In Chapter 6 our aim is to make use of the information on the local behaviour of the solution near the corner point, in order to design local meshing subordinate to the asymptotics.

## 4.1 Solution of Navier-Stokes equations in the axisymmetric case

The asymptotic behaviour of *plane flow* with corner singularities has been studied e.g. by Kondratiev [22], Ladevéze, Peyret [26], Kufner, Sändig [25]. The asymptotics of the biharmonic equation for the stream function $\psi$ are basic.

In this chapter we investigate *the pipe flow* (axisymmetric). We utilize the stream function - vorticity formulation of Navier-Stokes equations, which in cylindrical geometry reads

$$\frac{\partial\omega}{\partial t} + u_1\frac{\partial\omega}{\partial z} + u_2\frac{\partial\omega}{\partial r} + u_2\frac{\omega}{r} = \nu\left(\frac{\partial^2\omega}{\partial z^2}+\frac{\partial^2\omega}{\partial r^2}+\frac{1}{r}\frac{\partial\omega}{\partial r}-\frac{\omega}{r^2}\right), \tag{4.1}$$

$$\frac{\partial^2\psi}{\partial z^2}+\frac{\partial^2\psi}{\partial r^2}-\frac{1}{r}\frac{\partial\psi}{\partial r} = -r\omega , \tag{4.2}$$

$$u_1 = \frac{1}{r}\frac{\partial\psi}{\partial r}, \qquad u_2 = -\frac{1}{r}\frac{\partial\psi}{\partial z} , \tag{4.3}$$

where $r, z$ are cylindrical coordinates, $u_1 = V_z, u_2 = V_r$ are in turn axial and radial velocity components, $\omega$ is the vorticity, $\psi$ is the stream function, and $\nu$ is the viscosity. We assume that all derivatives exist here at least in the generalized sense.

First we study the *steady flow.* Putting $\omega, u_1, u_2$ from (4.2) – (4.3) into (4.1) we get

$$\begin{aligned}
&\frac{1}{r}\frac{\partial\psi}{\partial r}\frac{\partial}{\partial z}\Big(-\frac{1}{r}\frac{\partial^2\psi}{\partial z^2}-\frac{1}{r}\frac{\partial^2\psi}{\partial r^2}+\frac{1}{r^2}\frac{\partial\psi}{\partial r}\Big) - \frac{1}{r}\frac{\partial\psi}{\partial z}\frac{\partial}{\partial r}\Big(-\frac{1}{r}\frac{\partial^2\psi}{\partial z^2}-\frac{1}{r}\frac{\partial^2\psi}{\partial r^2}+\frac{1}{r^2}\frac{\partial\psi}{\partial r}\Big) - \\
&\qquad - \frac{1}{r^2}\frac{\partial\psi}{\partial z}\Big(-\frac{1}{r}\frac{\partial^2\psi}{\partial z^2}-\frac{1}{r}\frac{\partial^2\psi}{\partial r^2}+\frac{1}{r^2}\frac{\partial\psi}{\partial r}\Big) = \\
&= \nu\Big\{\frac{\partial^2}{\partial z^2}\Big(-\frac{1}{r}\frac{\partial^2\psi}{\partial z^2}-\frac{1}{r}\frac{\partial^2\psi}{\partial r^2}+\frac{1}{r^2}\frac{\partial\psi}{\partial r}\Big)+\frac{\partial^2}{\partial r^2}\Big(-\frac{1}{r}\frac{\partial^2\psi}{\partial z^2}-\frac{1}{r}\frac{\partial^2\psi}{\partial r^2}+\frac{1}{r^2}\frac{\partial\psi}{\partial r}\Big) + \\
&\qquad + \frac{1}{r}\frac{\partial}{\partial r}\Big(-\frac{1}{r}\frac{\partial^2\psi}{\partial z^2}-\frac{1}{r}\frac{\partial^2\psi}{\partial r^2}+\frac{1}{r^2}\frac{\partial\psi}{\partial r}\Big)+\frac{1}{r^3}\frac{\partial^2\psi}{\partial z^2}+\frac{1}{r^3}\frac{\partial^2\psi}{\partial r^2}-\frac{1}{r^4}\frac{\partial\psi}{\partial r}\Big\}.
\end{aligned} \tag{4.4}$$

We are interested in the asymptotic behaviour of the solution near the corners. One example of our solution domain is shown in Figure 4.1, where the corners are the points $P$, $Q$.

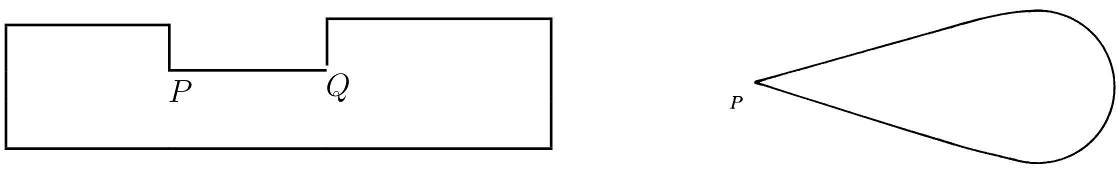


Fig. 4.1: The solution domain $\Omega$ (left) and the auxiliary domain $\Omega_0$ (right)

## 4.2 Asymptotics of steady Navier-Stokes flow near the corner

Substituting

$$z - z_0 = x, \qquad r - r_0 = y, \tag{4.5}$$

into (4.4) we come to the equation

$$\begin{aligned} -\frac{1}{(y+r_0)^2}\frac{\partial\psi}{\partial y}\frac{\partial^3\psi}{\partial x^3} - \frac{1}{(y+r_0)^2}\frac{\partial\psi}{\partial y}\frac{\partial^3\psi}{\partial x\partial y^2} + \frac{1}{(y+r_0)^3}\frac{\partial\psi}{\partial y}\frac{\partial^2\psi}{\partial x\partial y} + \\ + \frac{1}{(y+r_0)^2}\frac{\partial\psi}{\partial x}\frac{\partial^3\psi}{\partial x^2\partial y} + \frac{1}{(y+r_0)^2}\frac{\partial\psi}{\partial x}\frac{\partial^3\psi}{\partial y^3} - \frac{1}{(y+r_0)^4}\frac{\partial\psi}{\partial x}\frac{\partial\psi}{\partial y} &= \\ = \nu\,\{\frac{1}{y+r_0}(\frac{\partial^4\psi}{\partial y^4} + 2\frac{\partial^4\psi}{\partial y^2\partial x^2} + \frac{\partial^4\psi}{\partial x^4}) - \\ -\frac{1}{(y+r_0)^2}(\frac{\partial^3\psi}{\partial x^3} + \frac{\partial^3\psi}{\partial x^2\partial y} + \frac{\partial^3\psi}{\partial x\partial y^2} + \frac{\partial^3\psi}{\partial y^3}) + \frac{3}{(y+r_0)^3}\frac{\partial^2\psi}{\partial x^2} - \frac{3}{(y+r_0)^4}\frac{\partial\psi}{\partial x}\}, \end{aligned} \tag{4.6}$$

which, to be a bit more general, we consider on the domain $\Omega_0$ shown in Figure 4.1, the corner being in the origin of the coordinates, with the internal angle $\omega,\ 0 < \omega \le 2\pi$.

The coefficients in (4.6) are infinitely differentiable in $\Omega_0$. To study the asymptotic behaviour of the solution of (4.6) near the corner $P$, we first restrict ourselves (cf. Kondratiev [22]) to the principal part of equation (4.6), namely

$$\frac{\partial^4\psi}{\partial x^4} + 2\frac{\partial^4\psi}{\partial x^2\partial y^2} + \frac{\partial^4\psi}{\partial y^4} \;=\; f, \tag{4.7}$$

where we first assume $f = 0$. We perform the transformation into the polar coordinates $\rho, \vartheta$,

$$x = \rho\ \cos\vartheta, \qquad y = \rho\ \sin\vartheta. \tag{4.8}$$

Equation (4.7) in polar coordinates reads

$$\begin{aligned} S_0(\psi) \equiv \Big[\frac{1}{\rho}\frac{\partial}{\partial\rho}\rho\frac{\partial}{\partial\rho}\frac{1}{\rho}\frac{\partial}{\partial\rho}\rho\frac{\partial\psi}{\partial\rho} + \frac{1}{\rho}\frac{\partial}{\partial\rho}\rho\frac{\partial}{\partial\rho}\frac{1}{\rho^2}\frac{\partial^2\psi}{\partial\vartheta^2} \\ + \frac{1}{\rho^2}\frac{\partial^2}{\partial\vartheta^2}\frac{1}{\rho}\frac{\partial}{\partial\rho}\rho\frac{\partial\psi}{\partial\rho} + \frac{1}{\rho^2}\frac{\partial^2}{\partial\vartheta^2}\frac{1}{\rho^2}\frac{\partial^2\psi}{\partial\vartheta^2}\Big] = 0. \end{aligned} \tag{4.9}$$

The boundary conditions are

$$\psi\Big|_{\partial\Omega_0} = 0, \qquad \frac{\partial\psi}{\partial n}\Big|_{\partial\Omega_0} = 0 \tag{4.10}$$

where $n$ is the outgoing normal to the boundary $\partial\Omega$.

The problem (4.9), (4.10) is the same as in Kondratiev [23], and we follow his procedure. To study the asymptotics in $\Omega_0$ near the corner $P$, we first consider the infinite cone $\widetilde{\Omega}_0$,

$$\widetilde{\Omega}_0 = \{(\rho,\vartheta),\ 0 < \rho < \infty,\ \alpha < \vartheta < \beta\}, \tag{4.11}$$

where $\alpha \in <0, 2\pi),\ \beta \in (0, 2\pi>,\ \alpha < \beta$, are given angles, $\beta - \alpha = \omega$. Substituting $\tau = \ln\frac{1}{\rho}$ into (4.9), we get

$$[(\psi_{\tau\tau\tau\tau} + 4\psi_{\tau\tau\tau} + 4\psi_{\tau\tau}) + 4\psi_{\tau\vartheta\vartheta} + 2\psi_{\tau\tau\vartheta\vartheta} + \psi_{\vartheta\vartheta\vartheta\vartheta} + 4\psi_{\vartheta\vartheta}] \;=\; 0 \tag{4.12}$$

on the infinite strip $\tau \in (-\infty, +\infty)$ , $\vartheta \in (\alpha, \beta)$. Now we can perform the Fourier transform with respect to $\tau$, (i being the imaginary unit)

$$\widehat{\psi}(\lambda,\vartheta) = (2\pi)^{-1/2}\int_{-\infty}^{+\infty} e^{-\mathrm{i}\lambda\tau}\psi(\tau,\vartheta)d\tau, \tag{4.13}$$

and then Eq. (4.12) transforms to the ordinary differential equation

$$\widehat{L}(\vartheta,\mathrm{i}\lambda)\widehat{\psi} \equiv \widehat{\psi}_{\vartheta\vartheta\vartheta\vartheta} + (-2\lambda^2 + 4\mathrm{i}\lambda + 4)\widehat{\psi}_{\vartheta\vartheta} + (\lambda^4 - 4\mathrm{i}\lambda^3 - 4\lambda^2)\widehat{\psi} \;=\; 0, \tag{4.14}$$

where $\vartheta \in (\alpha, \beta)$. The operator $\widehat{L}$ depends analytically (in fact polynomially) on $\lambda$. Thus the inverse operator $R(\lambda)$ (if it exists at least for one point $\lambda \in \mathbb{C}$) is a meromorphic operator-valued function of $\lambda$, each pole of $R(\lambda)$ having finite multiplicity.

Equation (4.14) is a fourth order equation with constant coefficients. We denote them

$$A = -2\,\lambda^2 + 4\,\mathrm{i}\,\lambda + 4, \qquad B = \lambda^4 - 4\,\mathrm{i}\,\lambda^3 - 4\lambda^2.$$

To find the general solution of (4.14), we have to solve the biquadratic equation

$$\mu^4 + A\mu^2 + B = 0. \tag{4.15}$$

The squares of the solutions of Eq. (4.15) are $(\mu^2)_1 = \lambda^2$, $(\mu^2)_2 = (\lambda - 2\mathrm{i})^2$. So the solutions of (4.15) are

$$\mu_{1,2} = \pm\lambda, \qquad \mu_{3,4} = \pm(\lambda - 2\mathrm{i}). \tag{4.16}$$

Now we can prove the following Lemma.

**Lemma 4.1** *There are no poles of the resolvent $R(\lambda)$ on the line* $\mathrm{Im}\lambda = 2$.

Now we can use the following theorem proved by Kondratiev [23]. We use the Sobolev spaces $\mathring{\mathrm{W}}^k_\delta(\Omega)$ supplied with the norm

$$\|u\|^2_{\mathring{\mathrm{W}}^k_\delta(\Omega)} = \sum_{m=0}^{k} \iint_\Omega \rho^{\delta-2(k-m)}\,|D^m u|^2\,dx,\ D^m = \frac{D^{|m|}}{\partial x_1^{m_1}\partial x_2^{m_2}},\ |m| = m_1 + m_2. \tag{4.17}$$

Now let us return to the full Navier-Stokes equation (4.6). We rewrite (4.6) in the form

$$\frac{\partial^4\psi}{\partial y^4} + 2\frac{\partial^4\psi}{\partial y^2\partial x^2} + \frac{\partial^4\psi}{\partial x^4} \;=\; f, \tag{4.18}$$

where now

$$\begin{aligned} f \;&=\; \frac{1}{\nu}\,\{\frac{1}{(y+r_0)}\left(\frac{\partial^3\psi}{\partial x^3} + \frac{\partial^3\psi}{\partial x^2\partial y} + \frac{\partial^3\psi}{\partial x\partial y^2} + \frac{\partial^3\psi}{\partial y^3}\right) + \frac{3}{(y+r_0)^2}\frac{\partial^2\psi}{\partial x^2} - \frac{3}{(y+r_0)^3}\frac{\partial\psi}{\partial x}\} \;+ \\ &+\; \frac{1}{\nu}\,\{-\frac{1}{(y+r_0)}\frac{\partial\psi}{\partial y}\frac{\partial^3\psi}{\partial x^3} - \frac{1}{(y+r_0)}\frac{\partial\psi}{\partial y}\frac{\partial^3\psi}{\partial x\partial y^2} + \frac{1}{(y+r_0)^2}\frac{\partial\psi}{\partial y}\frac{\partial^2\psi}{\partial x\partial y} + \\ &+\; \frac{1}{(y+r_0)}\frac{\partial\psi}{\partial x}\frac{\partial^3\psi}{\partial x^2\partial y} + \frac{1}{(y+r_0)}\frac{\partial\psi}{\partial x}\frac{\partial^3\psi}{\partial y^3} - \frac{1}{(y+r_0)^3}\frac{\partial\psi}{\partial x}\frac{\partial\psi}{\partial y}\,\}. \end{aligned} \tag{4.19}$$

By (4.19) we get, cf. Agmon et al.[1], $\psi \in W^4(\widetilde{\Omega}_0 \cap \{(x,y), x^2+y^2 > R\})\ \forall R > 0$. As in Kondratiev, Olejnik [24], we can then receive $\psi \in \mathring{\mathrm{W}}^4_4(\widetilde{\Omega}_0)$. Then, using boundedness of $\frac{\partial\psi}{\partial x}$, $\frac{\partial\psi}{\partial y}$ in $\widetilde{\Omega}_0$ we can prove that the function $f$ in (4.19) satisfies $f \in \mathring{\mathrm{W}}^0_2(\widetilde{\Omega}_0)$.

Now we are in the position to use the following theorem by Kondratiev, Olejnik [24].

**Theorem 4.1** *Let $f \in \mathring{W}^{k_1}_{\delta_1}(\widetilde{\Omega}_0)$ and let $\psi \in \mathring{W}^{k+4}_{\delta}(\widetilde{\Omega}_0)$ be the solution of (4.7) satisfying the boundary conditions (4.10) on $\partial\widetilde{\Omega}$. Let*

$$h_1 \equiv \frac{-\delta_1 + 2k_1 + 6}{2} > \frac{-\delta + 2k + 6}{2} \equiv h\ ,\ k_1 \geq k. \tag{4.20}$$

*Suppose that the resolvent function $R(\lambda)$ has no poles on the line* $\mathrm{Im}\ \lambda = h_1$.

*Then the solution $\psi$ has the form*

$$\psi(x,y) = \sum_j \sum_{s=0}^{p_j - 1} a_{js}\rho^{-i\lambda_j}\ln^s\rho\cdot\psi_{sj}(\vartheta) \;+\; w(x,y), \tag{4.21}$$

*where $w$ satisfies (4.10), $w \in \mathring{W}^{k_1+4}_{\delta_1}(\widetilde{\Omega}_0)$, $\psi_{sj} \in C^\infty(\widetilde{\Omega}_0)$, $a_{js} = const.$, and $\lambda_j$ are the poles of multiplicity $p_j$ of the function $R(\lambda)$, satisfying $h < \mathrm{Im}\lambda_j < h_1$.*

Now we can apply Theorem 4.1 to Eq. (4.18), with $k = 0,\ \delta = 4$. We put $h_1 = 2$ according to Lemma 4.1, $k_1 = 0,\ \delta_1 = 2$.

Theorem 4.1 deals with the infinite cone $\widetilde{\Omega}_0$. The situation is a bit more complicated in the conical domain $\Omega_0$, and we refer to [5].

Now we try to find the poles of $R(\lambda)$. According to (4.16), the general solution of (4.14) is

$$\widehat{\psi} \ = \ c_1 \exp(\lambda\vartheta) + c_2 \exp(-\lambda\vartheta) + c_3 \sin(2\vartheta) + c_4 \cos(2\vartheta). \tag{4.22}$$

The boundary conditions are

$$\begin{aligned} \widehat{\psi}\Big|_{\vartheta=\alpha} &= 0, \qquad \widehat{\psi}\Big|_{\vartheta=\beta} = 0, \\ \frac{\partial\widehat{\psi}}{\partial\vartheta}\Big|_{\vartheta=\alpha} &= 0, \qquad \tfrac{\partial\widehat{\psi}}{\partial\vartheta}\Big|_{\vartheta=\beta} = 0, \end{aligned} \tag{4.23}$$

To obtain a nontrivial solution of the problem (4.22), (4.23), the necessary and sufficient condition is that the following determinant be zero,

$$R(\lambda) \equiv \det \begin{pmatrix} \exp(\lambda\alpha) & \exp(\lambda\beta) & \lambda\ \exp(\lambda\alpha) & \lambda\ \exp(\lambda\beta) \\ \exp(-\lambda\alpha) & \exp(-\lambda\beta) & -\lambda\ \exp(-\lambda\alpha) & -\lambda\ \exp(-\lambda\beta) \\ \sin(2\alpha) & \sin(2\beta) & 2\ \cos(2\alpha) & 2\ \cos(2\beta) \\ \cos(2\alpha) & \cos(2\beta) & -2\ \sin(2\alpha) & -2\ \sin(2\beta) \end{pmatrix} \ = \ 0. \tag{4.24}$$

Let us for example take the angle $\omega = \frac{3}{2}\pi$, i.e. $\alpha = 0,\ \beta = \frac{3}{2}\pi$. We come to the first root of (4.24): $\mathrm{i}\lambda_1 = -1.54448374$, which is simple, so that, according to Theorem 4.1, the first term of the asymptotic expansion is $\rho^{1.54448374}$, i.e.

$$\psi(\rho,\vartheta) = \rho^{1.54448374}\ \phi(\vartheta)\ +\ \dots\ . \tag{4.25}$$

This result is the same as that obtained in desk geometry by Kondratiev [23], Ladevéze, Peyret [26], M. Dauge [16], where

$$\psi^{desk}(\rho,\vartheta) = \rho^{1.5445}\ \phi^{d}(\vartheta)\ +\ \dots\ . \tag{4.26}$$

Now according to (4.3) we get the expansion for the velocities:

$$u_l(\rho,\vartheta) = \rho^{0.54448374}\varphi_l(\vartheta) + \dots,\ \ l = 1, 2, \tag{4.27}$$

where the functions $\varphi_l$ do not depend on $\rho$.

# 5 A posteriori error estimates for the Stokes equation

At present various a posteriori error estimates for the Stokes problem are available. We mention e.g. Babuška, Rheinboldt [3], Ainsworth, Oden [2], Verfürth [30]. Other references in [6].

One of the goals of this chapter is to study the aspect of the constant that appears in the estimate because it plays significant role in the adaptive mesh refinement. That is why we derive our own a posteriori estimate and trace carefully the role of different constants and their sources. In [6] we derived an a posteriori estimate for the Stokes problem in a 2-dimensional polygonal domain. In [7] we presented a posteriori estimates also for 3-dimensional domains.

The outline of the chapter is as follows. In Section 5.1 we consider the Stokes problem and its finite element approximation with Taylor-Hood elements. The a posteriori error estimate for the Stokes problem is shown in Section 5.2. In Sections 5.3-5.4 we describe implementation and tests of a posteriori error estimates of the discretization error for Navier-Stokes equations. These estimates are computed using approximate numerical solution on an initial finite element mesh. On each element they give us information about the discretization error. This enables us to consider the quality of the mesh, and also to refine the elements of the mesh, where the discretization error is too high, and then compute new solution on that new mesh. This way we can continue, until the prescribed accuracy is reached. Numerical results are demonstrated in Section 5.5 on a model of fluid flow in a domain with corner singularity.

## 5.1 The Stokes problem and finite element solution

Let us consider the steady Stokes problem on a bounded Lipschitzian domain $\Omega \subset I\!R^2$ as defined in Section 2.3, now with simplified boundary conditions: given $\boldsymbol{f} \in L^2(\Omega)$, find $\{\boldsymbol{u}, p\} \in H^1(\Omega)^d \times L_0^2(\Omega)$ such that, in the weak sense,

$$\begin{aligned} -\nu\Delta\boldsymbol{u} + \nabla p &= \boldsymbol{f} \ \text{ in } \Omega \ , \\ \text{div } \boldsymbol{u} &= 0 \ \text{ in } \Omega \ , \\ \boldsymbol{u} &= \boldsymbol{0} \ \text{ on } \partial\Omega \ , \end{aligned} \tag{5.1}$$

$L_0^2(\Omega)$ is the space of $L^2$ functions having mean value zero. Let us denote $(.,.)_0$ the scalar product in $L^2$, and let $V = H_0^1(\Omega)^2 \times L_0^2(\Omega)$. Problem (5.1) is known to have a unique solution, cf. [19], and consists in: find $\{\boldsymbol{u}, p\} \in V$ such that

$$\nu(\nabla\boldsymbol{u}, \nabla\boldsymbol{u}_*)_0 - (p, \text{div } \boldsymbol{u}_*)_0 + (p_*, \text{div } \boldsymbol{u})_0 \ = (\boldsymbol{f}, \boldsymbol{u}_*)_0 \quad \forall\{\boldsymbol{u}_*, p_*\} \in V. \tag{5.2}$$

For the finite element approximation we take $\Omega$ a polygon in $I\!R^2$, for simplicity. Let $\{\mathcal{T}_h\}_{h\to 0}$ be a regular (cf. [19]) family of triangulations of $\Omega$.

We use Hood-Taylor elements as defined in Chapter 3.

## 5.2 A posteriori error estimate for the Stokes problem

We define the residual components on the elements $K \in \mathcal{T}^h$, by the relations

$$\boldsymbol{R}_1(\boldsymbol{u}^h, p^h) = \boldsymbol{f} + \nu\Delta\boldsymbol{u}^h - \nabla p^h, \quad R_2(\boldsymbol{u}^h, p^h) = \text{div } \boldsymbol{u}^h. \tag{5.3}$$

The error components are defined on $\Omega$ by

$$\boldsymbol{e}_u = \boldsymbol{u} - \boldsymbol{u}^h \ , \ e_p = p - p^h \ ,$$

where $\{\boldsymbol{u}, p\}$ is the exact solution defined in (5.1), $\{\boldsymbol{u}^h, p^h\}$ is the approximate solution, by (4). The V norm of $\{\boldsymbol{e}_u, e_p\}$ is

$$\|\{\boldsymbol{e}_v, e_p\}\|_V^2 = (\boldsymbol{e}_u, \boldsymbol{e}_u)_1 + (e_p, e_p)_0.$$

Using the Poincaré-Friedrichs inequality, the Galerkin orthogonality, the Schwarz inequality, the interpolation properties of $V_h, \ Q_h$, and the estimate of the solution of the dual problem, we get the theorem (proof in [6] is based on the ideas of Eriksson et al. [18], and Babuška, Rheinboldt [3])

**Theorem 5.1** *Let $\Omega$ be a polygon in $I\!R^2$ with Lipschitz continuous boundary. Let $\mathcal{T}^h$ be a regular family of triangulations of $\Omega$. Let $\{\boldsymbol{u}^h, p^h\}$ be the Hood-Taylor approximation of the solution $\{\boldsymbol{u}, p\}$ of the Stokes problem. Then the error $\{\boldsymbol{e}_u, e_p\}$ satisfies the following a posteriori estimate*

$$\begin{aligned}\|\boldsymbol{e}_u\|_1 + \|e_p\|_0 \;\le\; 2\; C_P\; C_I\; C_R \sum_{K\in\mathcal{T}^h} \Bigg( & h_K \|\boldsymbol{R}_1(\boldsymbol{u}^h, p^h)\|_{0,K} + \\ & + \|R_2(\boldsymbol{u}^h, p^h)\|_{0,K} + h_K^{\frac{1}{2}} \sum_{l\in\partial K} \left\| \frac{1}{2} \left[\!\!\left[ \nu \frac{\partial \boldsymbol{u}^h}{\partial \boldsymbol{n}} \right]\!\!\right]_l \right\|_{0,l} \Bigg) ,\end{aligned} \tag{5.4}$$

*where $C_P, C_I, C_R$ are positive constants.*

**Remarks** The constants $C_P, C_I$, and $C_R$ in Theorem 5.1 come in turn from the Poincaré inequality, the interpolation properties of $V_h, Q_h$, and the regularity of the dual problem, respectively.

Our result in Theorem 5.1 is in agreement with that of Verfürth [30], though the technique of the proof is different, and we do not require any regularity.

## 5.3 A posteriori estimates for 2D steady Navier-Stokes equations

Let us consider the steady Navier-Stokes problem (4.6), (2.13), with boundary conditions (2.10), (2.11). For the discretization by finite elements we use again Hood-Taylor elements P2/P1.

Suppose that exact solution of the problem is denoted by $(u_1, u_2, p)$ and the approximate finite element solution by $(u_1^h, u_2^h, p_h)$. The exact solution differs from the approximate solution in the error

$$(e_{u_1}, e_{u_2}, e_p) \equiv (u_1 - u_1^h, u_2 - u_2^h, p - p_h). \tag{5.5}$$

For the solution $(u_1, u_2, p)$ we denote

$$\begin{aligned}\mathcal{U}^2(u_1,u_2,p,\Omega) &\equiv \|(u_1,u_2,p)\|_V^2 \equiv \|(u_1,u_2)\|_{1,\Omega}^2 + \|p\|_{0,\Omega}^2 \\ &\equiv \int_\Omega \left( u_1^2 + u_2^2 + \left(\frac{\partial u_1}{\partial x}\right)^2 + \left(\frac{\partial u_1}{\partial y}\right)^2 + \left(\frac{\partial u_2}{\partial x}\right)^2 + \left(\frac{\partial u_2}{\partial y}\right)^2 \right) \mathrm{d}\Omega + \int_\Omega p^2 \mathrm{d}\Omega.\end{aligned} \tag{5.6}$$

The estimate in Theorem 1 can be generalized to the Navier-Stokes equations:

$$\|(e_{u_1}, e_{u_2})\|_{1,\Omega}^2 + \|e_p\|_{0,\Omega}^2 \le \mathcal{E}^2(u_1^h, u_2^h, p^h), \tag{5.7}$$

where (cf. [30])

$$\mathcal{E}^2(u_1^h, u_2^h, p^h, \Omega) \equiv C \left[ \sum_{K\in\mathcal{T}^h} h_K^2 \int_{T_K} \left(r_1^2 + r_2^2\right) + \sum_{K\in\mathcal{T}^h} \int_{T_K} r_3^2 \mathrm{d}\Omega \right], \tag{5.8}$$

where $h_K$ denotes the diameter of the element $T_K$ and $r_i,\ i = 1,2,3,$ are the residuals

$$r_1 = f_x - \left( u_1^h \frac{\partial u_1^h}{\partial x} + u_2 \frac{\partial u_1^h}{\partial y} \right) + \nu \left( \frac{\partial^2 u_1^h}{\partial x^2} + \frac{\partial^2 u_1^h}{\partial y^2} \right) - \frac{\partial p^h}{\partial x}, \tag{5.9}$$

$$r_2 = f_y - \left( u_1^h \frac{\partial u_2^h}{\partial x} + u_2^h \frac{\partial u_2^h}{\partial y} \right) + \nu \left( \frac{\partial^2 u_2^h}{\partial x^2} + \frac{\partial^2 u_2^h}{\partial y^2} \right) - \frac{\partial p^h}{\partial y}, \tag{5.10}$$

$$r_3 = \frac{\partial u_1^h}{\partial x} + \frac{\partial u_2^h}{\partial y}. \tag{5.11}$$

Let us note that due to our practical experience we use only the element residuals.

Denote also

$$\mathcal{E}^2(u_1^h, u_2^h, p^h, T_K) \equiv C \left[ h_K^2 \int_{T_K} \left(r_1^2 + r_2^2\right) + \int_{T_K} r_3^2 \mathrm{d}\Omega \right]. \tag{5.12}$$

Qualitatively the value of the constant $C$ is not simple to determine, the sources are seen in Theorem 5.1. It is important, that $C$ doesn't depent on the mesh size and so can be determined experimentally for general situation.

By computing of the estimates (11) we obtain absolute numbers, that will depend on given quantities in different problems. We are mainly interested in the error related to the computed solution, i.e. relative error. This is given by the ratio of absolute norm of the solution error, related to unit area of the element $T_K$, $\frac{1}{|T_K|}\ \mathcal{E}^2(u_1^h, u_2^h, p^h, T_K)$, and the solution norm on the whole domain $\Omega$, related to unit area $\frac{1}{|\Omega|}\ \|(u_1^h, u_2^h, p^h)\|_{V,\Omega}^2$, i.e.

$$\mathcal{R}^2(u_1^h, u_2^h, p^h, T_K) = \frac{|\Omega|\ \mathcal{E}^2(u_1^h, u_2^h, p^h, T_K)}{|T_K|\ \|(u_1^h, u_2^h, p^h)\|_{V,\Omega}^2}. \tag{5.13}$$

## 5.4 Determination of the constant C

In papers [11], [12] we investigated the problem of the constant $C$ in the a posteriori error estimates. Comparing analytical and finite element solution of some model problems we found the apropriate value of the constant. For details we refer to [11] and [12].

## 5.5 Numerical results and application of estimates to the construction of adaptive meshes

Consider two-dimensional flow of viscous, incompressible fluid described by Navier-Stokes equations in domain with corner singularity, cf. Fig. 5.1.

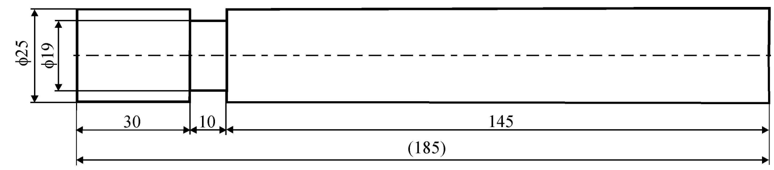


Fig. 5.1: Geometry of the channel

Due to symmetry, we solve the problem only on half of the channel, cf. Fig. 5.2. On the inflow we consider parabolic velocity profile, at the outflow 'do nothing' boundary condition. On the upper wall, no-slip condition and on the lower wall, condition of symmetry (i.e. only $y-$ component of velocity equals zero). We consider the following parameters: $\nu = 0.0001$ m$^2$/s, $u_{in} = 1$ m/s. The initial mesh is in Fig. 5.2. Relative errors on the elements of the initial mesh are on Fig. 5.3.

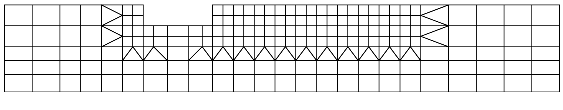

Fig. 5.2: Initial finite element mesh

Elements, where the relative error by (5.13) exceeds 3 % are refined, and new solution together with new error estimates is computed. The refinements are seen on Figures 5.4, 5.5.

The relative errors in the vicinity of the corner are shown on Figure 5.6. Numerical results of velocity components and pressure are on Figures 5.7 , 5.8, and 5.9. The corner singularities caused by nonconvex corners are approximated with high accuracy.

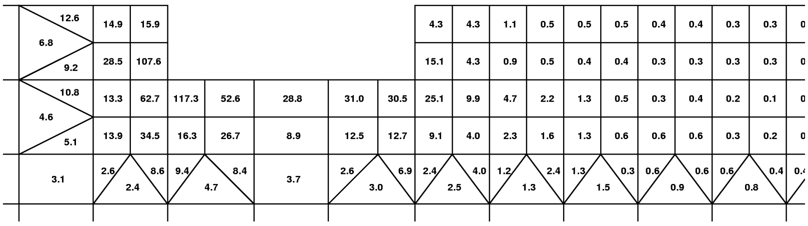

Fig. 5.3: Relative errors on elements of initial mesh

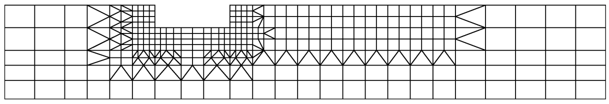

Fig. 5.4: Finite element mesh after first refinement

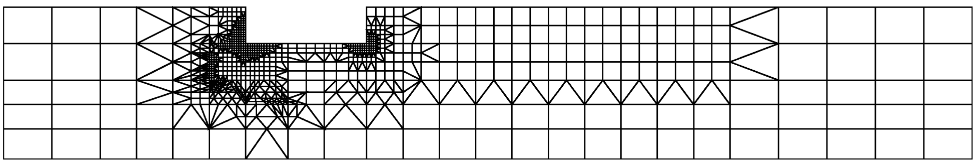

Fig. 5.5: Finite element mesh after third refinement

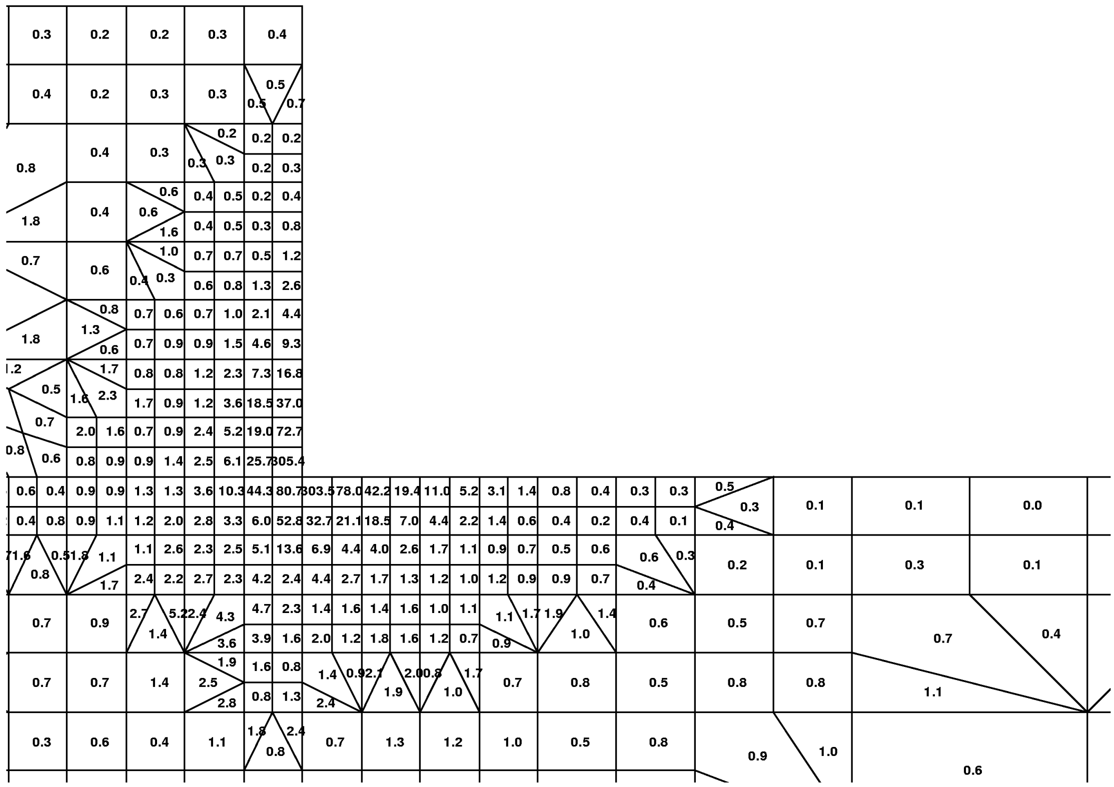

Fig. 5.6: Relative errors on elements of the third refinement

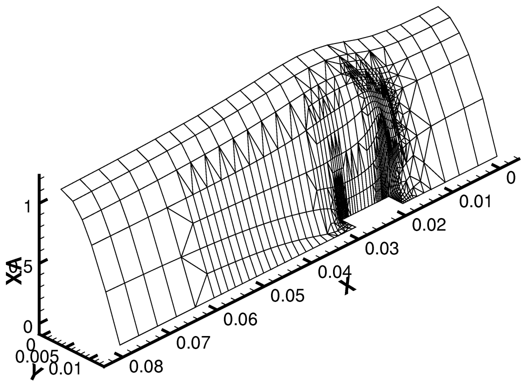


Fig. 5.7: Velocity $u_x$ after third refinement

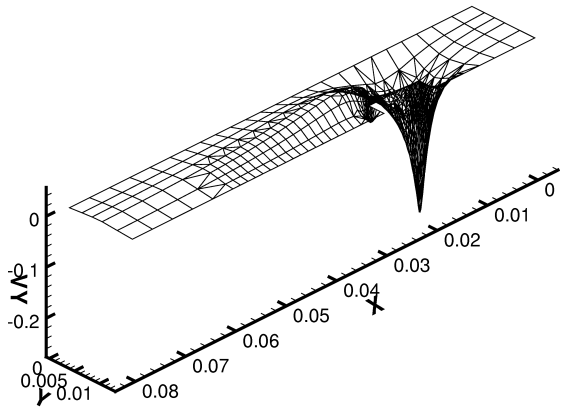


Fig. 5.8: Velocity $u_y$ after third refinement

## 5.6 Conclusions

In the a posteriori estimate (5.4) only the constant $C_P$ can be evaluated directly. The others are not known from the analysis. But in the application to the adaptive mesh refinement we need the constant. We developed a technique for calculating the constant with high accuracy. Of course this approach needs some improvement, and it will be a subject of future research.

Let us note that another way of local mesh refinement near the singularity has been suggested in [5]. This approach will be applied in Chapter 6.

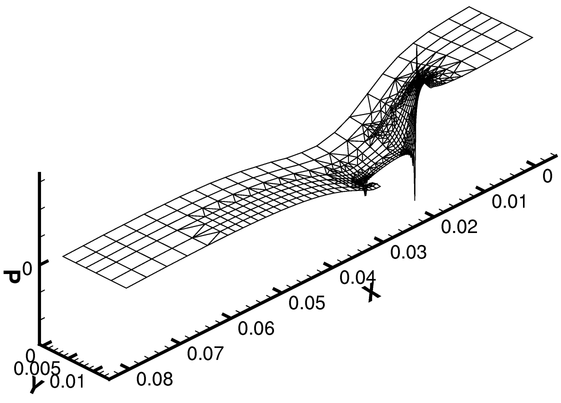


Fig. 5.9: Pressure p after third refinement

# 6 Application of a priori error estimates for Navier-Stokes equations

The goal of this chapter is to summarize author's experience with the application of a priori error estimates of the finite element method in computational fluid dynamics. This approach is applied to generation of the computational mesh in the purpose of uniform distribution of error on elements and is used in precise solution on domains with corner-like singularities. Incompressible viscous flow modelled by the steady Navier-Stokes equations (2.20)-(2.22) is considered.

One possible way to improve accuracy of solution by the FEM is to refine the mesh near places, where singularity can appear by means of adaptive refinement based on a posteriori error estimates or error estimators, as presented in Chapter 5. This method could be quite time demanding, since it needs several runs of solution. Completely different method is applied in this chapter. Computational mesh is prepared before the first run of the solution.

Numerical results are presented for flows in a channel with sharp obstacle and in a channel with sharp extension. Let us note that some other results were published in [14]

## 6.1 Algorithm for generation of computational mesh

In the derivation of the algorithm, two main 'tools' are used. The first is a priori estimate of the finite element error for the Navier-Stokes equations (2.20)-(2.22) (cf. [19])

$$\|\nabla(\mathbf{u}-\mathbf{u_h})\|_{L_2(\Omega)} \leq C\Big[\Big(\sum_K h_K^{2k} \mid \mathbf{u} \mid^2_{H^{k+1}(T_K)}\Big)^{1/2} + \Big(\sum_K h_K^{2k} \mid p \mid^2_{H^k(T_K)}\Big)^{1/2}\Big] \tag{6.1}$$

$$\|p-p_h\|_{L_2(\Omega)} \leq C\Big[\Big(\sum_K h_K^{2k} \mid \mathbf{u} \mid^2_{H^{k+1}(T_K)}\Big)^{1/2} + \Big(\sum_K h_K^{2k} \mid p \mid^2_{H^k(T_K)}\Big)^{1/2}\Big] \tag{6.2}$$

where $h_K$ is the diameter of triangle $T_K$ of a triangulation $\mathcal{T}$, and $k = 2$ for Hood-Taylor elements, which are applied in presented numerical experiments.

The second tool is the asymptotic behaviour of the solution near the singularity. In Section 4.2 (see also [5]), it was proved for the Stokes flow in axisymmetric tubes, that for internal angle $\alpha = \frac{3}{2}\pi$, the leading term of expansion of the solution for each velocity component is

$$u_i(\rho,\vartheta) = \rho^{0.5445}\varphi_i(\vartheta) + \ldots,\ i = 1,2 \tag{6.3}$$

where $\rho$ is the distance from the corner, $\vartheta$ the angle and $\varphi_i$ is a smooth function. The same expansion is known to apply to the plane flow (cf. [22]), and similar results were also proved for the Navier-Stokes equations. Differentiating by $\rho$, we observe $\frac{\partial u_i(\rho,\vartheta)}{\partial\rho} \to \infty$ for $\rho \to 0$.

Taking into account the expansion (6.3), we can estimate

$$\mid \mathbf{u} \mid^2_{H^{k+1}(T_K)} \approx C \int\limits_{r_K-h_K}^{r_K} \rho^{2(\gamma-k-1)}\ \rho\, d\rho = C\ \Big[-r_K^{2(\gamma-k)} + (r_K-h_K)^{2(\gamma-k)}\Big] \tag{6.4}$$

where $r_K$ is the distance of element $T_K$ from the corner, cf. Figure 6.1.

Putting estimate (6.4) into the a priori error estimate (6.1) or (6.2), we derive that we should guarantee

$$h_K^{2k}\Big[-r_K^{2(\gamma-k)} + (r_K-h_K)^{2(\gamma-k)}\Big] \approx h_{ref}^{2k} \tag{6.5}$$

in order to get the error estimate of order $O(h_{ref}^k)$ uniformly distributed on elements. From this expression, we compute element diameters using the Newton method in accordance to chosen $h_{ref}$. Similar idea was presented by C. Johnson for an elliptic problem in [21].

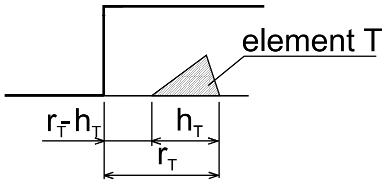


Fig. 6.1: Description of element variables

| $i$ | $r_i$ (mm) | $h_i$ (mm) |
|---|---|---|
| 1 | 0.25000 | 0.06004 |
| 2 | 0.18996 | 0.04808 |
| 3 | 0.14189 | 0.03795 |
| 4 | 0.10394 | 0.02947 |
| 5 | 0.07447 | 0.02245 |
| 6 | 0.05202 | 0.01674 |
| 7 | 0.03527 | 0.01217 |
| 8 | 0.02311 | 0.00858 |
| 9 | 0.01453 | 0.00584 |
| 10 | 0.00869 | 0.00380 |
| 11 | 0.00489 | 0.00234 |
| 12 | 0.00255 | 0.00134 |
| 13 | 0.00121 | 0.00070 |
| 14 | 0.00050 | 0.00050 |

| $i$ | $r_i$ (m) | $h_i$ (m) |
|---|---|---|
| 1 | 0.30000 | 0.06956 |
| 2 | 0.23044 | 0.05621 |
| 3 | 0.17423 | 0.04483 |
| 4 | 0.12940 | 0.03522 |
| 5 | 0.09419 | 0.02720 |
| 6 | 0.06699 | 0.02059 |
| 7 | 0.04640 | 0.01524 |
| 8 | 0.03116 | 0.01098 |
| 9 | 0.02017 | 0.00767 |
| 10 | 0.01250 | 0.00515 |
| 11 | 0.00735 | 0.00330 |
| 12 | 0.00405 | 0.00199 |
| 13 | 0.00206 | 0.00112 |
| 14 | 0.00094 | 0.00057 |
| 15 | 0.00038 | 0.00038 |

Table 6.1: Resulting refinement for the first (left) and the second (right) cases of geometry

## 6.2 Geometry and design of the mesh

The algorithm was applied to two different computational domains in 2D. The first is the channel with sudden intake of diameter (see Fig. 5.1), the second is the channel with abruptly extended diameter (Figure 6.2). Since these are symmetric, the problem was solved only on the upper half of the channels.

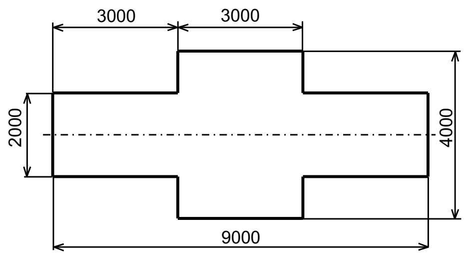


Fig. 6.2: The second geometry

In the first case of geometry, diameters of elements were computed for values $h_{ref} = 0.1732$ mm, $k = 2$, $\gamma = 0.5444837$. We started in the distance $r_1 = 0.25$ mm from the corner. This corresponds to cca 3% of relative error on elements. Fourteen diameters of elements were obtained (Table 6.1).

For the second channel, we used $h_{ref} = 0.1732$ m, $k = 2$, $\gamma = 0.5444837$ and started in the distance $r_1 = 300$ mm from the corner. Fifteen diameters of elements were obtained (Table 6.1).

Note, that those are '1D' data. An experiment with three meshes with different refined details (Figure 6.3) was performed (cf. [12],[28] for details). Type C of refinement in Figure

6.3 provided the best uniformity of the error on elements, therefore was chosen for further applications. This type of refinement corresponds to the polar coordinate system used in the derivation of the algorithm, and is applied in the two experiments described in this chapter.

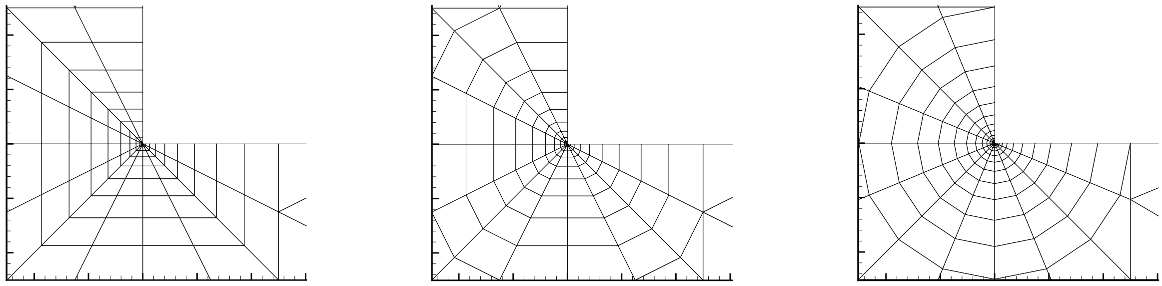

Fig. 6.3: Details of refined mesh - type A (left), type B (middle), type C (right)

The refined detail is connected to the rest of the coarse mesh. In Figures 6.4-6.5, final meshes after the refinement are shown for both geometries.

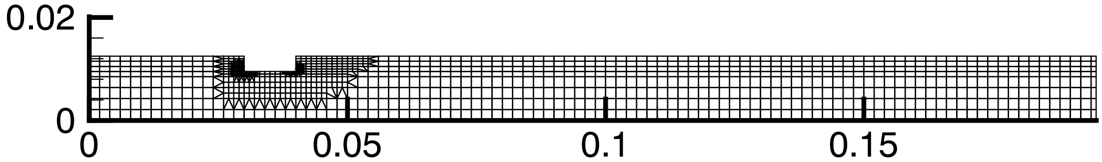


Fig. 6.4: Final computational mesh for the first channel

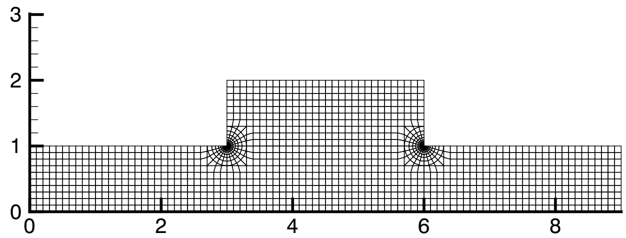


Fig. 6.5: Final computational mesh for the second channel

## 6.3 Measuring of error

To review the efficiency of the algorithm, we use a posteriori error estimates as derived in chapter 5, to evaluate the obtained error on elements. Suppose that the exact solution of the problem is denoted as $(u_1, u_2, p)$ and the approximate solution obtained by the FEM as $(u_1^h, u_2^h, p^h)$. The exact solution differs from the approximate solution in the error $(e_{u_1}, e_{u_2}, e_p) = (u_1 - u_1^h, u_2 - u_2^h, p - p^h)$.

In adaptive mesh refinement in Sections 5.3 - 5.5 we used the error estimator (5.13). In this Chapter, for the similarity with a priori error estimate, we use the modified absolute error defined as

$$\mathcal{A}_m^2(u_{1h}, u_{2h}, p_h, T_K, \Omega, n) = \frac{|\Omega| \mathcal{E}^2(u_{1h}, u_{2h}, p_h, T_K)}{|\overline{T_K}| \; \mathcal{U}^2(u_{1h}, u_{2h}, p_h, \Omega)} \tag{6.6}$$

where $|\overline{T_K}|$ is the mean area of elements obtained as $|\overline{T_K}| = \frac{|\Omega|}{n}$, where $n$ denotes the number of all elements in the domain, and the symbols $\mathcal{E}^2(u_{1h}, u_{2h}, p_h, T_K)$, $\mathcal{U}^2(u_{1h}, u_{2h}, p_h, \Omega)$ are dfefined in (5.6), (5.12).

## 6.4 Numerical results

**Channel with sudden intake of diameter** (results for Re = 1000)

In Figures 6.6-6.7, plots of entities that characterize the flow in the channel are presented. In Figure 6.6, there are streamlines and plot of velocity component $u_x$. Plots of velocity component $u_y$ and pressure are in Figure 6.7. Note, that the fluid flows from the right to the left on plots of $u_x$, $u_y$, and $p$, to have better view.

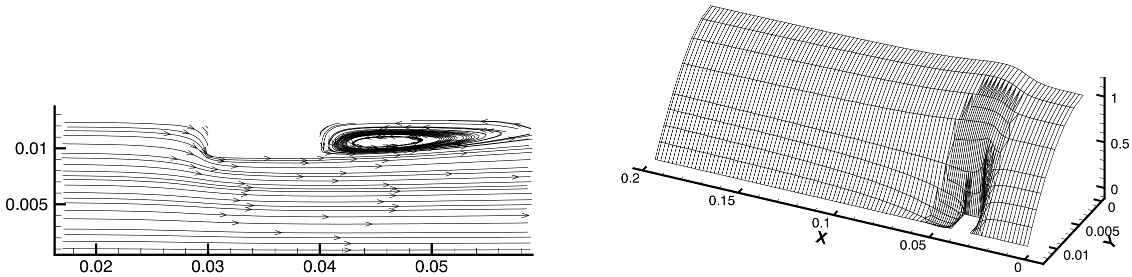


Fig. 6.6: Detail of streamlines (left) and velocity component $u_x$ (right)

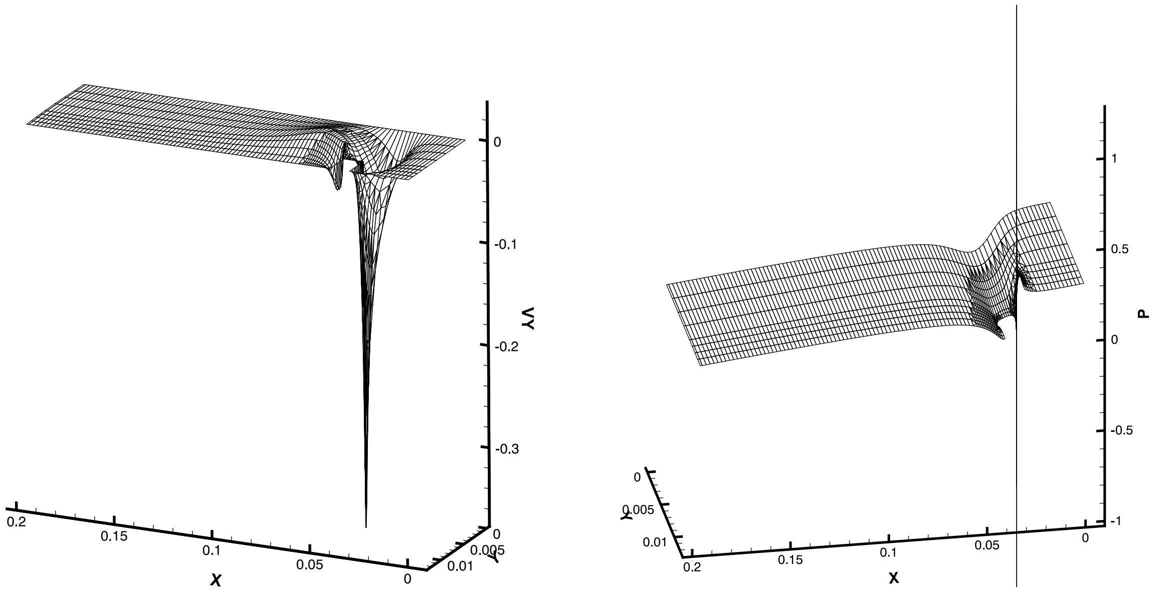


Fig. 6.7: Velocity component $u_y$ (left) and pressure (right)

In Figure 6.9, there are values of obtained error on elements in refined area. All values are listed in Table 6.2. Marking of elements in the table is described in Figure 6.8, together with plot of contours of velocity $u_y$ close to the corner.


Fig. 6.8: Contours of $u_y$ (left) and marking of elements for Table 6.2 (right)

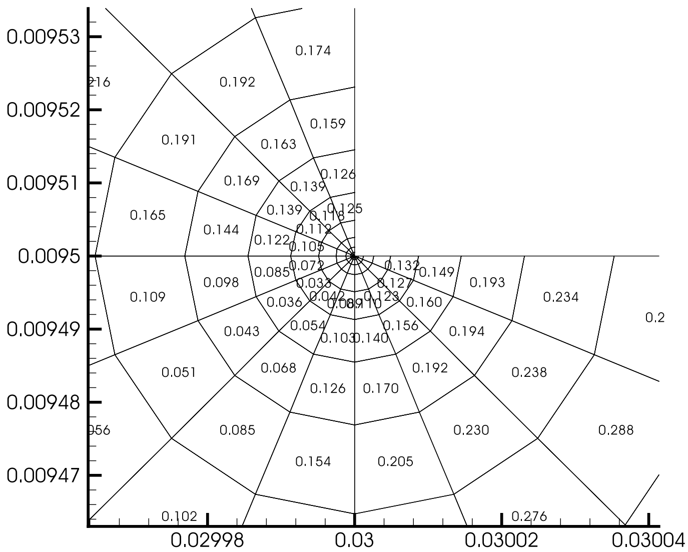


Fig. 6.9: FEM error on elements in the refined area for the first case of geometry

| | A | B | C | D | E | F | G | H |
|---|---|---|---|---|---|---|---|---|
| 1 | 1.858 | 0.652 | 0.229 | 0.103 | 0.132 | 0.149 | 0.193 | 0.234 |
| 2 | 2.221 | 0.664 | 0.135 | 0.105 | 0.127 | 0.160 | 0.194 | 0.238 |
| 3 | 2.427 | 0.513 | 0.122 | 0.103 | 0.123 | 0.156 | 0.192 | 0.230 |
| 4 | 2.292 | 0.407 | 0.110 | 0.095 | 0.110 | 0.140 | 0.170 | 0.205 |
| 5 | 1.574 | 0.261 | 0.083 | 0.069 | 0.087 | 0.103 | 0.126 | 0.154 |
| 6 | 0.523 | 0.104 | 0.034 | 0.037 | 0.042 | 0.054 | 0.068 | 0.085 |
| 7 | 0.585 | 0.093 | 0.032 | 0.030 | 0.033 | 0.036 | 0.043 | 0.051 |
| 8 | 1.544 | 0.274 | 0.079 | 0.064 | 0.072 | 0.085 | 0.098 | 0.109 |
| 9 | 2.223 | 0.404 | 0.115 | 0.091 | 0.105 | 0.122 | 0.144 | 0.165 |
| 10 | 2.409 | 0.521 | 0.126 | 0.098 | 0.112 | 0.139 | 0.169 | 0.191 |
| 11 | 2.277 | 0.654 | 0.134 | 0.101 | 0.118 | 0.139 | 0.163 | 0.192 |
| 12 | 1.912 | 0.665 | 0.237 | 0.102 | 0.125 | 0.126 | 0.159 | 0.174 |

| | I | J | K | L | M | N | con. | - |
|---|---|---|---|---|---|---|---|---|
| 1 | 0.283 | 0.345 | 0.399 | 0.499 | 0.530 | 0.793 | 1.222 | - |
| 2 | 0.288 | 0.341 | 0.408 | 0.482 | 0.596 | 0.782 | 1.380 | - |
| 3 | 0.276 | 0.329 | 0.392 | 0.476 | 0.570 | 1.353 | 2.495 | - |
| 4 | 0.245 | 0.289 | 0.343 | 0.390 | 0.471 | 0.577 | 1.996 | - |
| 5 | 0.185 | 0.216 | 0.242 | 0.252 | 0.222 | 0.499 | 1.754 | - |
| 6 | 0.102 | 0.120 | 0.122 | 0.142 | 0.151 | 0.419 | 1.813 | - |
| 7 | 0.056 | 0.066 | 0.082 | 0.126 | 0.388 | 1.070 | 3.776 | - |
| 8 | 0.124 | 0.140 | 0.168 | 0.194 | 0.363 | 0.896 | 1.733 | - |
| 9 | 0.189 | 0.215 | 0.243 | 0.268 | 0.309 | 0.488 | 0.957 | - |
| 10 | 0.216 | 0.245 | 0.265 | 0.285 | 0.277 | 0.610 | 1.558 | - |
| 11 | 0.212 | 0.237 | 0.237 | 0.284 | 0.411 | 1.021 | 2.786 | - |
| 12 | 0.199 | 0.186 | 0.209 | 0.172 | 0.311 | 0.496 | 1.970 | - |

Table 6.2: Obtained errors on elements for the first case of geometry

**Channel with abruptly extended diameter** (results for Re = 400)

Similarly, streamlines, plots of velocity components $u_x$ and $u_y$, and pressure are presented in Figures 6.10-6.11.

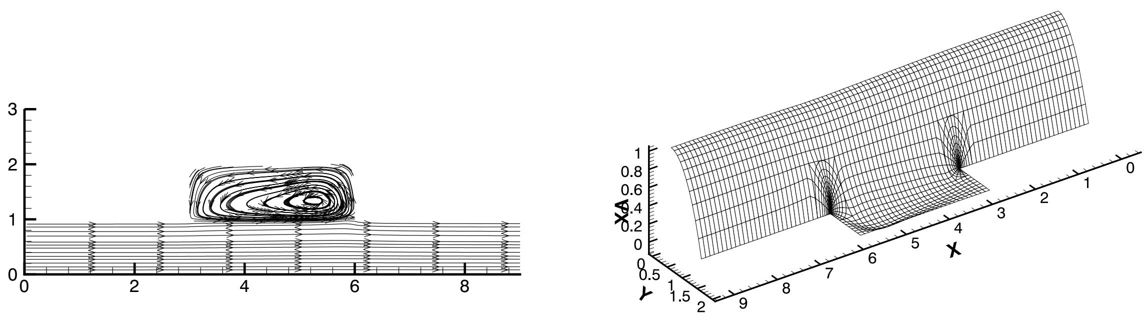


Fig. 6.10: Streamlines (left) and velocity component $u_x$ (right)

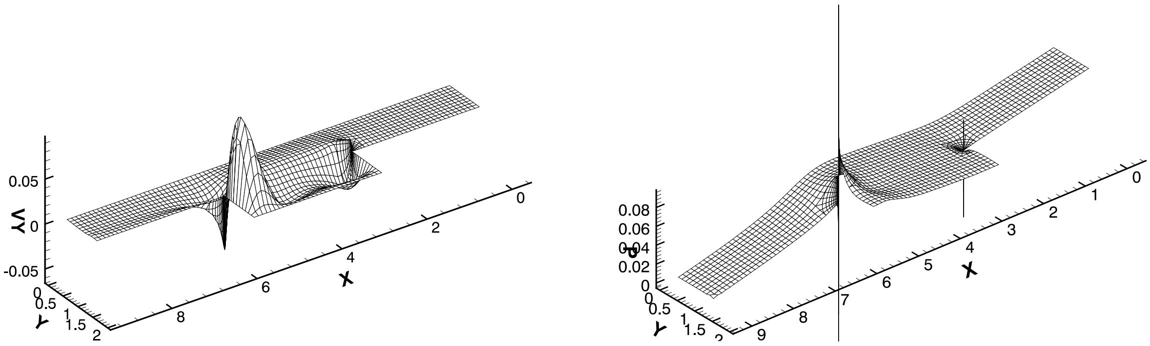


Fig. 6.11: Velocity component $u_y$ (left) and pressure (right)

In Figure 6.12, there are, again, values of obtained error on elements in refined area.

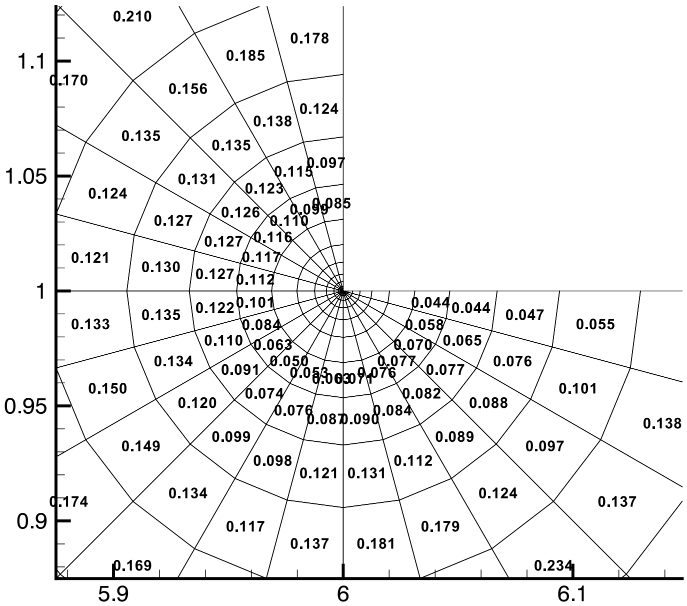


Fig. 6.12: FEM error on elements in the refined area for the second case of geometry

# 7 Conclusion

Presented work is mainly focused on flow problems with singularities caused by corners in the solution domain, and on the construction of the the FEM solution in the vicinity of these corners as precisely as desired.

We presented two ways for getting desired precision of the FEM solution in the vicinity of corners. Both make use of qualitative properties of the mathematical model of flow. As a mathematical model we accept the Navier-Stokes equations (NSE) for incompressible fluids.

The first approach described in Chapter 5 makes use of a posteriori error estimates of the FEM solution which is carefully derived to trace the quality of the solution. Especially the constant in the a posteriori estimate is investigated with care. Then we use the adaptive strategy to improve the mesh and thus to improve the FEM solution. Numerical results demonstrate the robustness of this approach.

The second approach stands on two legs. In Chapter 4 we derive the asymptotic behaviour of the exact solution of the NSE in the vicinity of the corner. This is obtained using some symmetry of the principal part of the Stokes equation, then applying the Fourier transform, and investigating the resolvent of the corresponding operator. Second leg is the a priori error estimate of the FEM solution where we estimate the seminorm of the exact solution by means of the above obtained asymptotics. In Chapter 6, according to these ideas we derive an algorithm for designing the FEM mesh in advance (a priori). On the mesh we then obtain the solution with desired precision, namely in the vicinity of the corner though there is a singularity there.

Two applications in Chapter 6 confirm the achievement of the goal – to obtain solution tinged with errors on elements satisfactorily small and uniformly distributed. The uniformity is apparent in Figures 6.9 and 6.12, and in Table 6.2. Using this approach, we can save a lot of computational time using mesh 'prepared' for expected solution.

At present we deal also with the stabilized version of FEM to enable the calculation of flows with higher Reynolds numbers [15]. In future we intend to combine stabilization with presented achievements on a posteriori error estimates. Our achievements with precise solution of problems with singularities may serve as an important tool for verification.

Results of Chapters 4 - 6 were presented e.g. on the following international conferences:

- FEF05, Finite Elements in Fluids, Swansea, March 2005, see [15]
- ICFD International Conference on Numerical Methods for Fluid Dynamics 2004, University of Oxford, March 29 – April 1, 2004, cf. [14]
- ICCFD3, Toronto, July 12 – 16, 2004, cf. [13]
- ENUMATH 2003, Prague, August 18 – 22, 2003, cf. [12]
- ICCFD2, 2-nd Int. Conf. on Computational Fluid Dynamics, Sydney, Australia, July, 2002,
- ENUMATH 2001, the 4-th European Conference on Numerical Mathematics and Advanced Applications, Ischia, Italy, July, 23 - 28, 2001,
- Finite Element Methods, Three-Dimensional Problems, Jyväskylä, June 2000
- ICCFD1, Int. Conf. on Computational Fluid Dynamics, Kyoto, JAPAN, July 2000
- Finite Element Methods, Supeconvergence, Post-Processing and A Posteriori Estimates, Jyvaskyla 1996, see [5]

# 8 References


[1] Agmon, S., Douglis, A., Nirenberg, L., Estimates near the boundary for solutions of elliptic partial differential equations satisfying general boundary conditions. I., Comm. Pure Appl. Math. **12**, 1959, 623-727.

[2] Ainsworth, M., Oden, J., T. (1997): A posteriori error estimators for the Stokes and Oseen problems. SIAM J. Numer. Anal., **34**, 228 - 245

[3] Babuška, I., Rheinboldt, W., C. (1978): A posteriori error estimates for the finite element method. Internat. J. Numer. Meth. Engrg., **12**, 1597 - 1615

[4] Brezzi, F., Fortin, M. *Mixed and Hybrid Finite Element Methods*, Springer, Berlin, 1991

[5] Burda, P. *On the FEM for the Navier-Stokes equations in domains with corner singularities.* In: Křížek, M., et al., editors. Finite Element Methods, Supeconvergence, Post-Processing and A Posteriori Estimates, Marcel Dekker, New York, 1998, 41-52

[6] Burda, P. (2000): An a posteriori error estimate for the Stokes problem in a polygonal domain using Hood-Taylor elements. In: Neittaanmäki, P., Tiihonen, T., and Tarvainen, P. (eds) ENUMATH 99, Proc. of the 3-rd European Conference on Numerical Mathematics and Advanced Applications. World Scientific, Singapore, 448 - 455

[7] Burda, P. *A posteriori error estimates for the Stokes flow in 2D and 3D domains.* In: Neittaanmäki, P., Křížek, M., editors. Finite Element Methods, 3D.(GAKUTO Internat. Series, Math. Sci. and Appl., Vol. 15), Gakkotosho, Tokyo, 2001, 34-44

[8] Burda, P., Kořenář, J. *Numerical solution of pulsatile flow in a round tube with axisymmetric constrictions.* In: COMMUNICATIONS, Vol. 19, Institute of Hydrodynamics, Prague, 1992, 87-110

[9] Burda, P., Kořenář, J., Numerical solution of Navier-Stokes equations for constricted pulsations, ZAMM **74** (1994), T649-T651.

[10] Burda, P., Kořenář, J., MAC scheme in the numerical solution of pulsatile flow, ICIAM Conf. Hamburg, 1995, ZAMM **76** (1996), S1, 365-366.

[11] Burda, P., Novotný, J., Sousedík, B. *A posteriori error estimates applied to flow in a channel with corners*, Mathematics and Computers in Simulation, **61** (2003), 375-383

[12] Burda, P., Novotný, J., Sousedík, B., Šístek, J. *Finite Element Mesh Adjusted to Singularities Applied to Axisymmetric and Plane Flow.* In: Feistauer M, et al., editors. Numerical Mathematics and Advanced Applications, ENUMATH 2003, Springer, Berlin, 2004, 186-195

[13] Burda, P., Novotný, J., Šístek, J. *Accurate solution of corner singularities in axisymmetric and plane flows using adjusted mesh of finite elements.* ICCFD3 Conference, Toronto, 2004, Book of Abstracts, 1-2, to appear in the Proceedings by Springer

[14] Burda, P., Novotný, J., Šístek, J., Precise FEM solution of corner singularity using adjusted mesh applied to axisymmetric and plane flow, ICFD Conf. on Num. Meth. for Fluid Dynamics, Univ. Oxford, March 2004, Int. J. Num. Meth. Fluids, **47**, 2005, pp. 1285 - 1292.

[15] P. Burda, J. Novotný, J. Šístek, On a modification of GLS stabilized FEM for solving incompressible viscous flows, Fef05, Swansea, March 2005, accepted by Int. J. Num. Meth. Fluids.

[16] Dauge, Monique, Stationary Stokes system in two or three dimensional domains with corners, Seminaire Equations aux Derivees Partielles 1987, expos, no. 10, Univ. de Nantes, 315-357.

[17] Douglas, J., Jr., Wang, J. *An absolutely stabilized Finite Element Method for the Stokes problem*, Math. Comp., **52** (1989), 495-508

[18] Eriksson, K., Estep, D., Hansbo, P., Johnson, C. (1995): Introduction to adaptive methods for differential equations. Acta Numerica,**1995**, CUP, 105–158.

[19] Girault, V., Raviart, P., G. *Finite Element Method for Navier-Stokes Equations*, Springer, Berlin, 1986

[20] Glowinski, R. *Finite Element Methods for Incompressible Viscous Flow*, Handbook of Numerical Analysis, Vol. IX, Elsevier, 2003

[21] Johnson, C. *Numerical Solution of Partial Differential Equations by the Finite Element Method*, Cambridge University Press, 1994

[22] Kondratiev, V., A. *Asimptotika rešenija uravnienija Nav'je-Stoksa v okrestnosti uglovoj točki granicy*, Prikl. Mat. i Mech., **1** (1967), 119-123

[23] Kondratiev, V. A., Krajevyje zadači dlja elliptičeskich uravněnij v oblasťach s koniěskimi i uglovymi točkami, Trudy Moskov. Mat. obshch. 16 (1967), 209 - 292.

[24] Kondratiev, V. A., Olejnik, O. A., Krajevyje zadači dlja uravněnij s častnymi proizvodnzmi v negladkich oblasťach, Uspechi Mat. Nauk 38 (1983), 3-76.

[25] Kufner, A., Sändig, Anna-Margarette, Some Applications of Weighted Sobolev Spaces, Teubner, Leipzig, 1987.

[26] Ladevéze J., Peyret, R., Calcul numérique d'une solution avec singularité des équations de Navier-Stokes: écoulement dans un canal avec variation brusque de section, Journal de Mécanique 13 (1974), 367-396.

[27] Skalák, Z., Numerical analysis of the flow in corrugated channels, Proc. Conf. Numerical Modelling Prague 1994, Eds. M. Feistauer, R. Rannacher, K. Kozel, FMF Prague 1995, 256-263.

[28] Šístek, J. *Solution of the fluid flow in a tube with singularity using suitable mesh refinement (in Czech).* In: Student Conference STČ 2003, ČVUT, Prague, 2003

[29] Šístek, J. *Stabilization of finite element method for solving incompressible viscous flows*, Diploma thesis, ČVUT, Praha, 2004

[30] Verfürth, R. (1996): A Review of A Posteriori Error Estimation and Adaptive Mesh-Refinement Techniques. Wiley and Teubner, Chichester

# 9 Curriculum Vitae

## Doc. RNDr. Pavel Burda, CSc.

- 1965 - 1970 studium na MFF KU Praha, obor numerická matematika
- 1970 - 1988 Ústav výpočtové techniky ČVUT (odborný asistent, ..., samostatný vědecký pracovník)
- 1978 - 1980 zastupující vedoucí Matematického oddělení Ústavu výpočtové techniky ČVUT (20 prac.)
- 1982 rigorozní zkouška na MFF KU Praha - RNDr.
- 1982 kandidát věd v oboru matematická analýza na MFF KU Praha
- 1987 samostatný vědecký pracovník
- 1988 - fakulta strojní ČVUT: katedra aplikované matematiky, ústav technické matematiky
- 1991 habilitace v oboru matematika
- 1992 docent na ústavu technické matematiky
- 1999 - vedoucí odboru aplikované a numer. matematiky (nyní 28 vědeckoped. prac.)

Narodil jsem se 14. ledna 1947 v Týně nad Vltavou. Jsem ženatý, mám dvě děti, manželka Kamila Burdová pracuje v Lékárně Novodvorská.

Vystudoval jsem v roce 1970 obor numerická matematika na Matematicko-fyzikální fakultě Karlovy university. Koncem 70-tých let jsem absolvoval aspiranturu v oboru matematická analýza. V roce 1981 jsem obhájil kandidátskou práci na téma "Nesamoadjungované problémy vlastních hodnot a jejich řešení metodou konečných prvků"

V roce 1988 jsem přešel s týmem 4 spolupracovníků na katedru aplikované matematiky strojní fakulty ČVUT. V roce 1991 jsem se habilitoval. Od roku 1999 přednáším v základním kursu (i v angličtině), na oboru Matematické modelování v technice, i v doktorském studiu. Od roku 2004 přednáším na Technické universitě v Liberci.

Účastním se významných mezinárodních konferencí, jak v zahraničí (např. MAFELAP Londýn, ICCFD: Kyoto, Sydney, Toronto, ICFD Oxford, FEM Jyvaskyla, ENUMATH, GAMM) tak u nás (např. Modelling, Česko-Francouzská konference), i domácích konferencí a seminářů (např. SAANM, PAANM, 3MI, Výpočtová mechanika).

Publikace: cca 110 publikací: 11 článků v zahraničních časopisech, 29 publikací ve sbornících z mezinárodních konferencí, 9 článků v českých časopisech, 45 publikací ve sbornících z domácích konferencí, 14 výzkumných zpráv, dvoje skripta.

Dva doktorandi už obhájili PhD disertace. Vedl jsem 4 diplomové práce a 1 bakalářskou. V současnosti vedu 5 doktorandů (jeden zahraniční), 2 diplomové práce na oboru Matematické modelování v technice.

Jako řešitel i spoluřešitel jsem vedl projekty podporované granty GAČR, GAAV, MŠMT, FRVŠ i interními granty ČVUT. V těchto projektech se významně účastní doktorandi a studenti. V roce 2005 jsem řešitelem grantu GAČR, grantu GAAV, spoluřešitelem grantu AV - Informační společnost, a 50 % kapacity se účastním na řešení výzkumného záměru.

Spolupracuji jak s domácími pracovišti akademickými (ÚH, ÚT, MÚ, FÚ), universitními (MFF, TUL, ZČU, VŠB TUO), tak zahraničními (Univ. Colorado at Denver, TH Darmstadt).

Jsem členem JČMF, CSTUG, GAMM.

Od r. 1999 jsem vedoucím odboru aplikované a numerické matematiky na Ústavu technické matematiky (28 vědeckopedagogických pracovníků). Jsem garantem PGS předmětu na fakultě strojní a na fakultě stavební a jsem členem oborové rady PGS na fakultě strojní. Jsem členem komise pro SZZ a komise pro obhajoby na ZČU Plzeň (zástupce MŠMT), člen komise pro doktorské zkoušky a obhajoby na FSv ČVUT (zástupce MŠMT).

Pracuji ve vědeckých výborech mezinárodních konferencí Modelling, ICCFD.

# Příloha

## Ke koncepci vědecké práce a výuky v oboru

V současné době vedu 5 doktorandů, dvě diplomové práce, vedu projekty na oboru Matematické modelování v technice. Přednáším pro doktorandy předmět Numerické řešení parciálních diferenciálních rovnic, základy metody konečných prvků, pro studenty oboru Matematické modelování v technice předmět Obyčejné a parciální diferenciální rovnice a předmět Metoda konečných prvků, jsem garantem těchto předmětů. V základním kursu na FS ČVUT přednáším předměty Matematika 3 a Numerická matematika (oboje i v angličtině). Na Technické universitě v Liberci mám přednášky předmětů Matematika 1 a Matematika 2 v základním kursu na fakultě mechatroniky.

### Výsledky ve výchově vědeckých pracovníků

A) PhD. získali:

- Ing. Alexandr Damašek
- RNDr. Eva Neumanová

B) Státní doktorskou zkoušku složil:

- RNDr. Vladislav Starý

C) v doktorském studiu:

- Ing. Pavel Moses
- Ing. Jakub Šístek
- RNDr. Marta Čertíková

D) v doktorském studiu v angličtině:

- Mgr. Omar Aleyan (Libye)

E) jako školitel specialista spolupracuji s prof. Markem při doktorském studiu:

- Ing. Bedřicha Sousedíka

### Výsledky pedagogické

A) Diplomové práce obhájili:

- Mgr. Jan Gregor (1988) na MFF KU v Praze
- Ing. Pavel Moses (2001) - 1. místo v soutěži diplomek o Zvoníčkovu nadaci
- Ing. Jakub Šístek (2005) - 1. místo v soutěži diplomek o Zvoníčkovu nadaci
- Ing. Martin Soukenka (2005) FJFI

B) Bakalářskou práci obhájil:

- Mgr. Michal Jelínek (2002) - nyní doktorand na Univ. Pensylvania

C) Studentská tvůrčí činnost:

- Pavel Moses, 4. roč. (2000) - 3. místo
- Bedřich Sousedík, 4. roč. (2000) - 4. místo
- Pavel Moses, 5. roč. (2001) - 1. místo
- Bedřich Sousedík, 5. roč. (2001) - 3. místo
- Jakub Šístek, 4. roč. (2003) - 6. místo
- Ing. Pavel Moses, doktorand (2004) - 5. místo
- Michal Rod, 5. roč. (2005) 1. místo

**Přehled externích grantů za 10 let, u nichž byl autor řešitelem nebo spoluřešitelem:**

1) GAČR - řešitel (**2005 - 2007**)
106/05/2731: Aplikace adaptivních víceúrovňových metod a metod dekompozice domén v proudění tekutin a nelineární pružnosti

2) AVČR Informační společnost - spoluřešitel (**2005 - 2008**)
(nositel: Ústav termomechaniky, řešitel: doc. Okrouhlík)
1ET400760509: Výzkum, testování, implementace a aplikace paralelních postupů pro modelování úloh mechaniky kontinua. Vytvoření elektronického výukového nástroje

3) GAAV - řešitel (2002 - **2005**)
IAA 2120201: Studium struktury úplavů při interakci těles s proudící tekutinou numerickými i optickými experimentálními metodami

4) GAČR - spoluřešitel (2002 - 2004)
GA 101/02/0391: Numerická simulace a experimentální výzkum aeroelasticity leteckých konstrukcí s uvážením velkých výchylek

5) FRVŠ - řešitel (2002)
2094/F4: Inovace předmětu Numerické řešení PDR a základy MKP

6) GAAV - řešitel (1998 - 2000)
A 2120801: Vývoj numerických metod pro řešení kmitání vlivem proudící tekutiny v lopatkových strojích

7) GAČR - spoluřešitel (1998 - 2000)
GA 201/98/0528: Řešení úloh s velkými řídkými soustavami lineárních a nelineárních algebraických rovnic

8) GAČR - spoluřešitel (1997 - 1999)
GA 101/97/0826: Hydroelastická interakce proudící tekutiny s pružnou stěnou kanálu (trubicí) s aplikacemi v biomechanice krevního oběhu

9) GAČR - spoluřešitel (1994 - 1996)
GA 101/94/0280: Teoretická analýza a numerické řešení dynamické interakce poddajného tělesa s proudící tekutinou

10) MŠMT Rozvoj vzdělávání - řešitel (1994 - 1995)
spolunositel: ÚH Praha, spoluřešitel RNDr. Z. Skalák)
PV 425/1994/VŠAV: Proudění v umělých cévních náhradách

**Výzkumné záměry**

1) J04/98/2/210000010 (MSM 210000010) - Aplikovaná matematika v technických vědách
řešitel prof. Kozel (1999 - 2004)

2) J04/98/2/210000003 (MSM 210000010) - řešitel prof. Bittnar (1999 - 2004)

3) MSM 684 0770010 - Aplikovaná matematika v technických a fyzikálních vědách
- řešitel prof. Kozel (**2005 - 2009**)
- účast: 50% kapacity